

THE PENNSYLVANIA STATE UNIVERSITY

SCHREYER HONORS COLLEGE

DEPARTMENT OF AEROSPACE ENGINEERING

**Characterizing Optimum Performance Range of
Electrodynamic Tether Systems using TeMPEST**

RITU BHALODIA

SPRING 2024

Submitted in Partial Fulfillment
of the Requirements
for a Baccalaureate Degree in Aerospace Engineering with Honors.

The dissertation of Ritu Bhalodia was reviewed and approved by the following:

Sven G. Bilén
Professor of Engineering Design,
Electrical Engineering, and Aerospace Engineering
Thesis Supervisor

Namiko Yamamoto
Associate Professor of Aerospace Engineering
Honors Adviser

ABSTRACT

The study focuses on addressing the escalating challenge in low Earth orbit (LEO) of orbital debris, non-functional satellites, space vehicle stages, and fragments resulting from collisions and explosions. Although there are over 25,000 pieces of debris exceeding 10 cm in diameter in LEO as of 2022, 50 derelict objects are identified as particularly concerning. Using the Linux-based simulation software, TeMPEST (TEthered Mission Planning and Evaluation Software Tool), this research simulates electrodynamic tether systems (EDTs) that feature long conducting tethers and, in some cases, energy storage modules, for the active deorbiting of these objects. By systematically varying EDT properties and orbital elements, the simulation aims to ascertain the optimal operational range for the tethered system. This insight, coupled with the understanding derived from Space Laws, will guide the identification of viable debris mitigation strategies, facilitating the targeted removal of the 50 most problematic debris objects from LEO.

Table of Contents

LIST OF FIGURES	iv
LIST OF TABLES	v
ACKNOWLEDGMENTS	vi
Chapter 1 Introduction	1
1.1 Overview	1
1.2 History of Tethers	3
1.3 Applications of Electrodynamic Tethers	7
1.3.1 Power Generation	7
1.3.2 Satellite Re-boost and Orbit Maneuvering	8
1.3.3 Radiation Belt Remediation	9
1.3.4 Interplanetary Transfer	9
1.3.5 Space Debris Mitigation	10
1.4 Modern Research into Debris Mitigation Using Tethers	10
1.4.1 Tether Robotic System	11
1.4.2 Tether Space Net	11
1.4.3 Tether Harpoon	12
1.5 Problem Statement	13
1.6 Thesis Overview	14
Chapter 2 Energy Harvesting using Space Debris Mitigation	15
2.1 Overview	15
2.2 Fundamentals of EDTs	17
2.3 Harvesting Energy	18
2.4 Energy and Power	20
2.4.1 Anode	21
2.4.2 Cathode	21
2.4.3 Load	22
2.4.4 Tether	22
2.4.5 Thrust	23
2.4.6 Storage Device	23
2.4.7 Total Electrical Power and Electrical Energy	23
Chapter 3 Tether Composition and Simulation Software	25
3.1 Composition of Tether System	25
3.1.1 Tether Insulation	26
3.1.2 Material Composition	27
3.1.3 Tether Geometry	28
3.1.4 Plasma Contactors	28
3.1.4.1 Thermionic Cathode Plasma Contactor	29
3.1.4.2 Hollow Cathode Plasma Contactor	29

3.1.4.3 Parker-Murphy Sphere	30
3.1.4.4 Field Emitter Cathode.....	30
3.1.4.5 Electron Cyclotron Resonance Plasma Contactor	30
3.1.4.6 Radio Frequency Plasma Contactor	30
3.1.5 End-mass	31
3.1.6 Energy Storage Devices	31
3.1.6.1 Batteries.....	32
3.1.6.2 Supercapacitors.....	32
3.1.6.3 Flywheels.....	32
3.1.6.4 Thermal Energy Storage.....	33
3.2 TeMPEST.....	33
3.2.1 History of TeMPEST	34
3.2.2 General Architecture	34
Chapter 4 Results and Analysis	36
4.1 System Concept.....	36
4.1.1 Tether	36
4.1.2 Orbital Parameters.....	37
4.1.3 Assumptions	39
4.2 Results.....	40
4.2.1 Mission Elapsed Time (Lifetime).....	40
4.2.2 Total Energy.....	41
4.2.3 Power.....	43
4.3 Summary	44
Chapter 5 Conclusion and Future Work	45
Bibliography	48
Appendix A Simulation Graphs.....	53
Appendix B Sample Parameters File	61

LIST OF FIGURES

Figure 1. Tethered Satellite System-1 (TSS-1) Mission [24]	2
Figure 2. Schematic of an Open-Cathode Hollow Contactor [28].....	22
Figure 3. Schematic of an Electrodynamic Tether operating in Earth’s magnetic field [29]...26	
Figure 4. Altitude versus mission elapsed time for Group1 orbit	41
Figure 5. Total energy versus mission elapsed time for various tether diameters for Group1 orbit	42
Figure 6. Total energy versus mission elapsed for various tether lengths for Group1 orbit....	43
Figure 7. Power as a function of mission elapsed time for Group1 orbit	44
Figure 8. Altitude versus mission elapsed time for Group1 orbit (Load resistance = 100 Ω) .53	
Figure 9. Energy versus mission elapsed time for Group1 orbit (Load resistance = 100 Ω)...54	
Figure 10. Energy versus mission elapsed time for Group2	55
Figure 11. Altitude versus mission elapsed time for Group2.....	56
Figure 12. Energy versus mission elapsed time for Group3	57
Figure 13. Altitude versus mission elapsed time for Group3.....	58
Figure 14. Energy versus mission elapsed time for Group4	59
Figure 15. Altitude versus mission elapsed time for Group4.....	60

LIST OF TABLES

Table 1. 50 SMC objects in the LEO orbit [19].....	16
Table 2. SMC objects distributed into four main groups	38

ACKNOWLEDGMENTS

I would like to express my deepest gratitude to Dr. Bilén and Dr. McTernan for their unwavering support and guidance throughout this journey. Their collective expertise, encouragement, and collaborative spirit have been invaluable, shaping the trajectory of my research and fostering an environment conducive to growth and innovation. I am profoundly thankful for their patience, insights, and camaraderie, which have undoubtedly enriched my academic and personal experience.

In addition, I am indebted to my mom and my sister for being constant wellsprings of inspiration and unwavering pillars of support. Their boundless love, encouragement, and belief in my abilities have propelled me forward during moments of doubt and adversity. Their resilience, determination, and unwavering faith in my pursuits serve as a constant reminder of the importance of perseverance and dedication in achieving one's goals.

To my mom and sister, and to my research group, I extend my heartfelt appreciation for your enduring support, encouragement, and belief in me. Your contributions, whether through words of encouragement, constructive feedback, or acts of kindness, have left an indelible mark on my journey, for which I am truly grateful.

Chapter 1

Introduction

1.1 Overview

To support space exploration, engineers and scientists continually seek innovative solutions to propel spacecraft, generate power, and mitigate space debris. Among these solutions, electrodynamic tethers (EDTs) emerge as an interesting technology, leveraging the fundamental principles of electromagnetism to achieve remarkable feats in propulsion, power generation, and orbital dynamics manipulation.

Fundamentally, an EDT is a thin, conductive wire stretching from a spacecraft that is used to harness energy by the motion of the system across the Earth's magnetic field. This innovative technology combines the elegant simplicity of electromagnetic induction with the complexities of space dynamics, offering a versatile platform for a myriad of space missions.

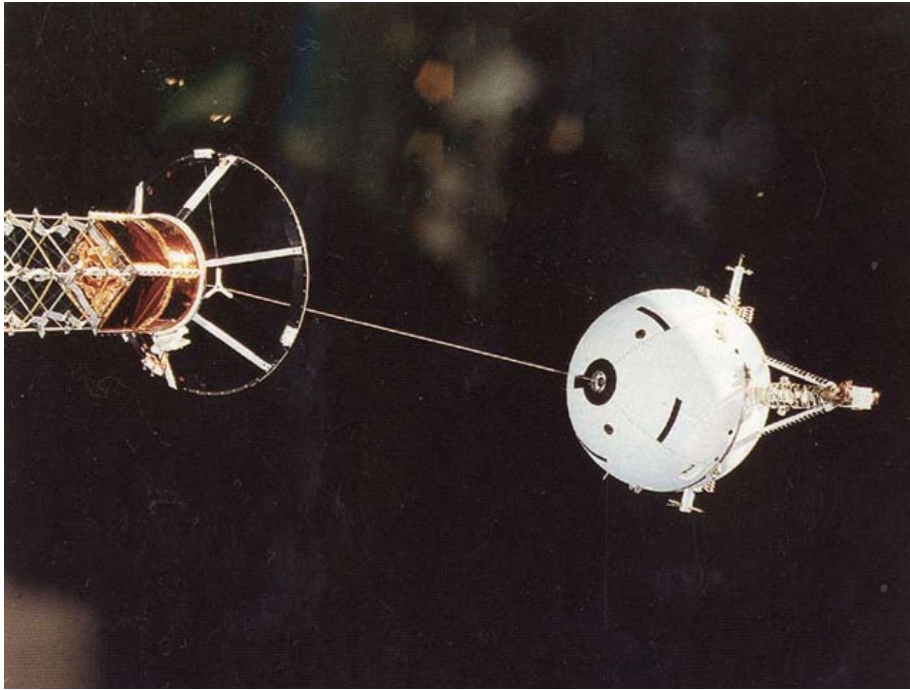


Figure 1. Tethered Satellite System-1 (TSS-1) Mission [24]

The principle underlying the functioning of EDTs lies in the interaction between the moving conductive tether and the magnetic field of the Earth. As the tether traverses through this magnetic field, it induces an electric current along its length through the process of electromagnetic induction. This current, in turn, interacts with the Earth's magnetic field, resulting in the generation of a force known as the Lorentz force. Utilizing the Lorentz force, EDTs offer unique capabilities in spacecraft propulsion, enabling precise maneuvers and orbit adjustments without the need for traditional rocket engines. By controlling the current flowing through the tether, engineers can control the thrust generated, providing significant control over spacecraft motion.

In addition to propulsion, EDTs have the potential to generate electricity in space by converting the kinetic energy of orbital motion into electrical power. As the tether moves

through Earth's magnetic field, it creates a flow of electrons that can be harvested for onboard power needs, offering a renewable energy source for space missions. Beyond propulsion and power generation, EDTs play a vital role in space debris mitigation efforts. By deploying tethers from spacecraft, it is possible to interact with defunct satellites and debris, altering their orbits and facilitating controlled re-entry into Earth's atmosphere, thus reducing the risk of collisions and clutter in space.

However, the realization of EDTs in space missions comes with its challenges, including material selection, deployment mechanisms, and environmental factors such as radiation and micrometeoroids. Overcoming these challenges requires meticulous planning and engineering expertise to ensure the reliability and effectiveness of EDT systems in space. In summary, EDTs represent a promising technology with diverse applications in space exploration. As researchers and engineers continue to refine EDT technology and address technical challenges, the potential for EDTs to revolutionize space missions and advance our understanding of the cosmos remains significant.

1.2 History of Tethers

Theoretical Foundations (1895-1970s)

Konstantin Tsiolkovsky introduced the concept of an orbital tower in 1895, drawing inspiration from the Eiffel Tower [1]. His vision entailed a colossal structure extending into space, featuring a "celestial castle" at its pinnacle. This tower, dubbed the "Tsiolkovsky Tower", would stretch from Earth's surface to geosynchronous orbit (GSO), serving as the foundation for tethered satellite systems (TSSs). Tsiolkovsky's proposal included a "Shuttle-borne Skyhook"

for low orbital research, utilizing excess centrifugal force beyond geosynchronous altitude to support the structure in tension. These pioneering ideas laid the groundwork for subsequent space elevator concepts that would enable payloads to traverse between Earth and space without propulsion.

Yuri Artsutanov, a Russian scientist, introduced a modern concept of space elevators in 1960, suggesting the use of a geostationary satellite as a base for deploying a downward-extending cable. This idea, presented to the Russian-speaking audience in an interview, involved lowering the cable from the satellite to the Earth's surface using a counterweight to maintain the cable's center of gravity motionless relative to Earth. Artsutanov also proposed tapering the cable's thickness to ensure constant tension, with the cable being thinner at ground level and thicker towards geostationary orbit [3].

In 1966, four American engineers—Isaacs, Vine, Bradner, and Bachus—reinvented the concept, naming it the “Sky-hook” [4]. Their analysis explored suitable materials for building a space elevator, revealing the substantial strength required, surpassing existing materials like graphite, quartz, and diamond.

Subsequently, Colombo et al. presented a concept for a shuttle-borne skyhook in 1974, which gained attention within the spaceflight engineering community through a technical paper by Pearson in 1975 [5]. Pearson's design included a tapered cross-section for the cable, with maximum thickness at geostationary orbit to accommodate greater tension and reduced thickness towards the tips to minimize weight per unit area. He also proposed extending a counterweight to 144,000 kilometers as the lower section of the elevator was constructed.

Alternative concepts emerged, such as Moravec's proposal for a non-synchronous orbital skyhook in 1977, which involved a rotating cable with its rotation speed matching the orbital speed to achieve zero instantaneous velocity at the point closest to Earth [6].

Discussions of anchored lunar satellites by Jerome Pearson in 1979 and the introduction of space elevators to a wider audience through Arthur C. Clarke's novel *The Fountains of Paradise* further fueled interest in the concept [7]. Subsequent works, including a historical account by Tiesenhausen in 1984 and studies on spinning systems by Carroll [25], contributed to the ongoing exploration and development of space elevator concepts.

In recent years, there has been a resurgence of interest in exploring various applications of space tethers, with researchers focusing on a wide array of possibilities. This heightened attention, especially over the past decade, underscores the significant potential of space tether technology. Some noteworthy applications include deploying and retrieving subsatellites, utilizing aerobraking techniques, employing electrodynamic boosts, facilitating satellite deorbiting, and conducting momentum transfer with careful analysis of libration and rotation dynamics.

Early Experiments (1960–1970s)

In the 1960s and 1970s, as space exploration gained momentum, researchers conducted initial experiments to validate space tether concepts. The first mission employing a space tether took place in 1966 during NASA's Gemini-11 mission, on which a 15-meter cable was utilized to link two capsules together. These early efforts provided valuable insights into the behavior of tethers in orbit but were limited in scope and duration.

Spaceflight Demonstrations of EDTs (1980–1990s)

The 1980s and 1990s marked a significant period of advancement for EDT technology, with the realization of spaceflight demonstrations and experiments. OEDIPUS-A launched in 1989 was the first electrodynamic tether was deployed from a sounding rocket to investigate the coupling between its ends while situated in the ionosphere. The tethered payload comprised two rotating sub-payloads weighing 84 kg and 131 kg respectively, connected by a spinning tether. This mission set a new record for the longest electrodynamic tether in space at the time, measuring 958 meters (3,143 feet) in length. NASA's Tethered Satellite System (TSS-1) mission in 1992 represented a major milestone, deploying a conductive tether from the Space Shuttle to study tether dynamics and plasma interactions in Earth's ionosphere. Although being deployed only 260 meters, the satellite demonstrated the feasibility of deploying, controlling, and retrieving the tether, showcasing the ease of control and unexpected stability of the tethered satellite. This EDT encountered a deployment mechanism jam and a deployment length of 256 m [8]. Despite encountering these technical challenges and an early termination of the mission, subsequent endeavors such as TSS-1R in 1996 continued to push the boundaries of EDT research.

Ongoing Research and Applications (2000s–Present)

In the 21st century, research into EDTs has persisted, fueled by advancements in materials science, spacecraft technology, and computational modeling. Space agencies and commercial entities alike have proposed EDTs for a variety of missions, including propulsion, power generation, and space debris mitigation. A recent tethered mission involves the Miniature Tether Electrodynamic Experiment (MiTEE) developed by the University of Michigan [9]. In

2015, NASA selected MiTEE as a University CubeSat Space Mission Candidate, and the project successfully delivered flight hardware. MiTEE was a CubeSat experiment designed to measure electrical current along a tether ranging from 10 to 30 meters (33 to 98 feet) in length. Its objective is to deploy a subsatellite, approximately $8\text{ cm} \times 8\text{ cm} \times 2\text{ cm}$ ($3.15\text{ in} \times 3.15\text{ in} \times 0.79\text{ in}$) in size, from a 3U CubeSat to assess satellite electrodynamic tethers in space. In January 2021, MiTEE-1 was launched into space as part of Virgin Orbit's LauncherOne test flight.

As our understanding of EDTs continues to deepen and technology advances, the potential applications of these innovative devices in shaping the future of space exploration remain vast and compelling.

1.3 Applications of Electrodynamic Tethers

Several modern research efforts are exploring the potential applications and technological advancements of EDTs in various space missions. Here are a few notable examples, along with their sources:

1.3.1 Power Generation

EDTs harvest energy via the principle of electromagnetic induction. As the tether moves through the Earth's magnetic field at orbital velocities, it generates an electric current along its length. This current can be collected and used to power onboard systems or stored for later use. Thus, electrodynamic tethers can be used to generate electrical energy using the orbital energy of the satellite and, hence, can be used to supplement or replace traditional solar power systems

onboard spacecraft, providing a continuous source of renewable energy even in the shadows of the Earth. But, there is a trade-off of orbital altitude, which will be covered in Chapter 2 in detail.

1.3.2 Satellite Re-boost and Orbit Maneuvering

Satellites in low-altitude orbits are constantly affected by the Earth's atmosphere, which can cause their orbits to decay over time. Traditionally, one can use a propulsion system that requires propellant to maintain the satellite's orbit, which is costly to transport and difficult to replenish. Tethers can offer a propellantless alternative by utilizing electrical current (usually collected via solar panels) to interact with the Earth's magnetic field, generating thrust without the need for traditional propellants. This approach essentially uses the planet's magnetic field as a reaction mass, providing a sustainable and efficient means of propulsion for satellite re-boosting [10]. Hence, EDTs can address another significant challenge, which is the need to re-boost satellites in space. Another concept study showed that a 10-km tether attached to the International Space Station (ISS) and utilizing about 10 kW of power from the ISS, could save about 80% of chemical propellant used for re-boosting it over a 10-year period, ultimately saving about US\$1 billion [11].

A multi-EDT system can be used for attitude stabilization, precise pointing, and orbit maneuvering purposes. Simulations have demonstrated that a chip satellite's ("ChipSat") attitude can be stabilized and orbital maneuvers performed simultaneously [12]. This multi-EDT ChipSat concept can be used for various missions such as maintaining sunpointing (using attitude controls) to increase the efficiency of solar cells.

1.3.3 Radiation Belt Remediation

Both satellites and humans are exposed to mission-threatening radiation from Van Allen Belts and, hence, it is necessary to safeguard both the crews and the payloads from exposure to these harmful radiating particles. One of the proposed ways to achieve it is using magnetic shielding, but this approach necessitates large masses and is only effective within specific frequency ranges. Fortunately, charged EDTs offer a promising alternative. These tethers are a high voltage electrostatic structure that could help in dispersing enough radiation belt particles, ultimately leading to remediating the radiation region while passing through it [13].

1.3.4 Interplanetary Transfer

The electric sail, or E-sail, operates by utilizing the solar wind—a stream of charged particles emitted by the Sun—as a means of propulsion for spacecraft. It consists of a set of long, thin, bare wires extending from the spacecraft, but is not efficient enough to power an electric thruster since weak superconductors are required. Instead, bare tethers could be used for efficiency purposes [14]. As the spacecraft moves through space, the electric fields generated by the charged tethers interact with the solar wind, creating a force known as the Lorentz force. This force transfers momentum to the spacecraft, propelling it forward without the need for traditional propellants. By adjusting the voltage applied to the tethers, spacecraft equipped with electric sails can control their trajectory and speed. Electric sails offer a promising propulsion method for long-distance space missions, as they rely on abundant solar wind particles for propulsion and do not require onboard fuel.

1.3.5 Space Debris Mitigation

Orbital debris, also known as space debris or space junk, refers collectively to defunct satellites, spent rocket stages, and other fragments left behind from human activities in space. These objects are in various Earth orbits, posing a significant threat to active satellites, spacecraft, and astronauts. Space tethers offer a potential solution to the growing problem of orbital debris. By deploying a tether-equipped spacecraft into orbit, it can intercept and capture debris, either by physically grappling with it or by using electrodynamic forces to alter its orbit. Once captured, the debris can be deorbited safely, allowing it to burn up in the Earth's atmosphere. This technology has the potential to mitigate the risks posed by space debris and ensure the long-term sustainability of space activities [15]. However, further research and development are needed to refine tether-based debris removal techniques and make them viable for practical implementation.

The next section delves into modern research in debris mitigation, exploring innovative approaches and emerging technologies aimed at addressing the challenges posed by orbital debris.

1.4 Modern Research into Debris Mitigation Using Tethers

The accumulation of debris has become a pressing concern, particularly in low Earth orbit (LEO), where collisions with debris can occur frequently. With over 25,000 pieces of debris larger than 10 cm in diameter in LEO as of 2022, efforts to mitigate the problem are crucial [26]. Strategies include tracking and monitoring debris, developing technologies for debris removal, and implementing guidelines for responsible space activities. Addressing the

challenge of orbital debris requires international collaboration and innovative solutions to ensure the sustainability of space exploration and satellite operations. Several potential research advancements have been made in technologies towards debris mitigation using tethers:

1.4.1 Tether Robotic System

In the context of capturing space debris using robotic arms, specialized robotic arm devices or autonomous modules are attached to tethered systems to perform the capture. Various designs for these arms, manipulators, and modules have been proposed in the literature, ranging from universal to target-specific designs. Functionally, these manipulators must securely grip the object and may include basic servicing functions to prevent the creation of secondary debris. The autonomous module can feature sensors, cameras, and thrusters. During the approach phase, the robotic module may operate in tight tether mode, using controlled tether deployment for maneuvering without consuming fuel. Once the target is grappled and stabilized, it can be transported along the tether, or the tether can be retracted into the active spacecraft for transportation. The development of space robotic arms and autonomous space robots is a dynamic field, with numerous projects proposing tethered robotic arms for space debris removal [16].

1.4.2 Tether Space Net

The concept of employing a space net for capturing non-cooperative space debris holds significant promise. This lightweight and compact net can be readily deployed using a simple

spring or explosive mechanism without prior stabilization of the target object. It possesses the capability to capture objects with complex shapes and can cover considerable distances to reach the target, facilitated by its connection to an active spacecraft through a long tether. To ensure stability, masses can be affixed to the net's edges, equipped with special mechanisms to tighten the net upon capturing the target. However, accurately predicting the motion of the net remains a key challenge in mission design. The process of space debris capture using a net involves several phases including ejection, deployment, capture, and closing. The utilization of a net for space debris capture was initially proposed and investigated within the framework of the European Space Agency's Robotic Geostationary Orbit Restorer project [17].

1.4.3 Tether Harpoon

A space tether harpoon is a device used to capture space debris by propelling a projectile attached to a tether toward the target object. Upon impact, the harpoon penetrates the debris, allowing it to be secured and potentially removed from orbit. The primary advantage of utilizing a harpoon lies in its simplicity; however, inaccuracies in aiming and unsuccessful shots can result in the twisting of the target object and the generation of secondary space debris. Furthermore, employing a harpoon may induce the spinning of the space debris target, necessitating subsequent stabilization during the post-capture stage. Simultaneously, the selection of the optimal point on the debris surface and the timing of the harpoon shot can facilitate the detumbling of the target. A study proposed the implementation of thrusters on the harpoon [18]. This study develops a detumbling control scheme based on the linear quadratic regulator, pulse-width pulse-frequency modulation, and particle swarm optimization.

It is worth noting that, while space debris presents significant challenges, innovative solutions are being explored to mitigate its impact. Technologies such as tether robotic systems, tether space nets, and tether harpoons offer promising avenues for debris removal. International collaboration and continued research efforts are essential to ensure the sustainability of space exploration and satellite operations. Furthermore, it is intriguing to consider the potential of space debris for energy harvesting. While still in the conceptual stages, these ideas highlight the potential for turning a challenge into an opportunity in the realm of space exploration and sustainability.

1.5 Problem Statement

Orbital debris poses a significant and escalating challenge in LEO, threatening active satellites and space missions. Despite numerous debris removal proposals, identifying effective strategies remains a pressing concern. This study aims to address this challenge by investigating the efficacy of EDTs using TeMPEST simulation software to deorbit the 50 statistically most hazardous derelict objects. The primary objective is to determine the optimal operational parameters of EDTs, considering various tether properties and orbital elements, to facilitate targeted removal of the most problematic debris objects. By integrating insights from simulation outcomes and space law principles, this research seeks to contribute to the development of practical and legally compliant debris mitigation strategies.

1.6 Thesis Overview

This thesis delves into the pressing issue of space debris accumulating in LEO, with a particular emphasis on the 50 most hazardous objects. It introduces EDTs as a promising solution to this problem in Chapter 2. Using advanced simulation software like TeMPEST, the research aims to optimize the operational parameters of EDTs for targeted debris removal. By systematically testing various EDT configurations and considering factors like orbital elements, and tether composition covered in Chapter 3, the study seeks to identify EDTs as an effective strategy for mitigating space debris while simultaneously harvesting energy. Subsequently, Chapter 4 describes the resulting configuration of EDT system that can be used for mitigating the debris identified in Chapter 2 by grouping them into groups with similar orbital parameters and debris mass. The final chapter of this research concludes the thesis and provides future work needed to be done in the advancement of this research.

Chapter 2

Energy Harvesting using Space Debris Mitigation

2.1 Overview

In 2021, a diverse group of international space organizations collectively published a process for identifying the debris in orbit that poses a potential risk to operational satellites and that needs to be remediated [19]. Table 1 shows the list of the top 50 statistically most concerning (SMC) objects narrowed down from the list of non-operational LEO objects available on Space-track.org using 11 different methods proposed in the article.

Table 1. 50 SMC objects in the LEO orbit [19]

SATNO	Number of Lists	SATNAME	APOGEE, km	PERIGEE, km	INCL, deg	MASS, kg	COUNTRY	LAUNCH
22,566	11	SL-16 R/B	848	837	71.0	9000	CIS	3/26/1993
22,220	10	SL-16 R/B	848	827	71.0	9000	CIS	11/17/1992
31,793	10	SL-16 R/B	846	843	71.0	9000	CIS	6/29/2007
26,070	9	SL-16 R/B	854	827	71.0	9000	CIS	March 2, 2000
16,182	10	SL-16 R/B	844	833	71.0	9000	CIS	10/22/1985
20,625	10	SL-16 R/B	853	834	71.0	9000	CIS	5/22/1990
27,006	8	SL-16 R/B	1006	986	99.5	9000	CIS	October 12, 2001
23,705	9	SL-16 R/B	852	831	71.0	9000	CIS	10/31/1995
25,407	9	SL-16 R/B	844	835	71.0	9000	CIS	7/28/1998
23,405	10	SL-16 R/B	845	838	71.0	9000	CIS	11/24/1994
17,974	9	SL-16 R/B	846	823	71.0	9000	CIS	5/13/1987
23,088	8	SL-16 R/B	845	841	71.0	9000	CIS	4/23/1994
22285	8	SL-16 R/B	844	840	71.0	9000	CIS	12/25/1992
22,803	8	SL-16 R/B	850	823	71.0	9000	CIS	9/16/1993
19,650	7	SL-16 R/B	848	831	71	9000	CIS	11/23/1988
24,298	8	SL-16 R/B	863	839	70.8	9000	CIS	April 9, 1996
28,353	7	SL-16 R/B	848	842	71.0	9000	CIS	October 6, 2004
17,590	8	SL-16 R/B	841	831	71.0	9000	CIS	3/18/1987
19,120	7	SL-16 R/B	842	814	71.0	9000	CIS	5/15/1988
25,400	7	SL-16 R/B	813	801	98.6	9000	CIS	October 7, 1998
27,386	5	ENVISAT	766	764	98.1	7800	ESA	January 3, 2002
27,001	6	METEOR 3 M	1013	994	99.6	2500	CIS	October 12, 2001
24,277	4	ADEOS	794	793	98.9	3560	JPN	8/17/1996
27,601	4	H-2A R/B	836	734	98.2	3000	JPN	12/14/2002
15,334	4	SL-12 R/B(2)	847	838	71.0	2440	CIS	9/28/1984
37,932	4	CZ-2D R/B	846	791	98.7	4000	PRC	11/20/2011
10,732	4	SL-8 R/B	995	966	82.9	1435	CIS	3/15/1978
24,279	5	H-2 R/B	1306	860	98.7	2700	JPN	8/17/1996
23,704	3	COSMOS 2322	854	842	71.0	3250	CIS	10/31/1995
21,090	3	SL-8 R/B	992	961	82.9	1435	CIS	May 2, 1991
28,352	3	COSMOS 2406	863	844	71.0	3250	CIS	October 6, 2004
23,087	2	COSMOS 2278	852	841	71.1	3250	CIS	4/23/1994
19,119	2	COSMOS 1943	851	833	71.0	3250	CIS	5/15/1988
27,597	2	ADEOS 2	801	800	98.5	3680	JPN	12/14/2002
25,861	4	SL-16 R/B	645	622	98.2	9000	CIS	7/17/1999
15,772	3	SL-12 R/B(2)	848	794	71.1	2440	CIS	5/30/1985
10,693	3	SL-8 R/B	989	957	83.0	1435	CIS	2/28/1978
17,973	2	COSMOS 1844	866	824	71.0	3250	CIS	5/13/1987
27,387	3	ARIANE 5 R/B	796	748	98.6	2575	FR	January 3, 2002
7594	3	SL-8 R/B	981	955	82.9	1435	CIS	12/26/1974
23,180	3	SL-8 R/B	992	950	82.9	1435	CIS	7/14/1994
10,138	3	SL-8 R/B	1001	970	82.9	1435	CIS	August 7, 1977
13,917	3	SL-8 R/B	996	954	82.9	1435	CIS	3/24/1983
13,719	3	SL-3 R/B	896	791	81.3	1100	CIS	12/14/1982
14,625	2	SL-8 R/B	999	969	82.9	1435	CIS	November 1, 1984
20,624	2	COSMOS 2082	856	833	71.0	3250	CIS	5/22/1990
12,092	2	SL-8 R/B	996	953	82.9	1435	CIS	October 12, 1980
9044	3	SL-8 R/B	988	966	83.0	1435	CIS	7/21/1976
12,504	2	COSMOS 1275	1014	954	83.0	800	CIS	April 6, 1981
16,292	3	SL-8 R/B	996	953	82.9	1435	CIS	11/28/1985

Notice that 84% of 50 SMC objects are of Russian (1992 onwards) or Soviet (through 1991) origin, i.e., Commonwealth of Independent States (CIS). The rest of the objects (16%) collectively come from China (2%), the European Space Agency (ESA) (6%), and Japan (8%). It

is interesting to note that 39 out of these 50 objects are rocket bodies (RBs) and the remaining 11 are payloads. As mentioned in Table 1, 40 of the top 50 SMC objects were launched before December 31, 2000, whereas the rest of them were abandoned from January 1, 2001. This study uses orbital data from the top 50 SMC objects to run simulations to ascertain the optimal operational range of EDTs.

2.2 Fundamentals of EDTs

As mentioned before, electrodynamic tethers (EDTs) utilize the interaction between a conductive tether and a planetary magnetic field to generate propulsion or harvest energy. Fundamentally, an EDT consists of a long, conductive wire deployed from a spacecraft or satellite. When the spacecraft moves through a planetary magnetic field, such as the Earth's, it induces an electric current along a conducting tether through electromagnetic induction. The fundamental principle of electromagnetic induction is to generate an electromotive force (EMF) or voltage in a conductor when it is exposed to a changing magnetic field.

In propulsion applications, the electric current flowing through the tether interacts with the magnetic field, resulting in a force known as the Lorentz force. The Lorentz force on a charged particle is given by

$$\vec{F}_L = q\vec{E}_{\text{tot}} , \quad (2.1)$$

where \vec{E}_{tot} is the induced electronic field given as

$$\vec{E}_{\text{tot}} = \vec{E} + \vec{v} \times \vec{B} . \quad (2.2)$$

This force develops an “open circuit” electric potential on the charge carriers in the tether as it crosses the magnetic field:

$$\varepsilon = \int_0^L \vec{E}_{\text{tot}} \cdot \vec{u} dl = \int_0^L (\vec{E} + \vec{v} \times \vec{B}) \cdot \vec{u} dl . \quad (2.3)$$

The surrounding plasma in the LEO orbit can help form a closed circuit between the two ends of the tether, allowing current to flow through the tether. The tether also experiences an electrodynamic force acting in the opposite direction of the velocity of the spacecraft due to the current flow, which is given by

$$\vec{F}_{\text{ed}} = \int_0^L \vec{I} \times \vec{B} dl . \quad (2.4)$$

This force imparts momentum to the spacecraft, causing it to accelerate or decelerate, depending on the direction of the current. Hence, by controlling the electric current, the spacecraft can adjust its orbit, perform station-keeping maneuvers, or even deorbit.

2.3 Harvesting Energy

Energy is neither created, nor destroyed, but can be converted from one form into another. There are four main energy sources that can be considered for a satellite in Earth's orbit:

1. Total orbital energy from potential and kinetic energy due to their orbit, E_{orb} ;
2. Electrical energy from electrical components that dissipate or inject power into the system, E_{elec} ;
3. Energy obtained from the atmospheric drag force on the satellite, E_{drag} ; and
4. The rotational kinetic energy of the earth, E_{earth} .

Thus, the total energy defined in an Earth-centered inertial (ECI) frame of the satellite system is

$$E_{\text{tot}} = E_{\text{orb}} + E_{\text{elec}} + E_{\text{earth}} + E_{\text{drag}} \quad (2.5)$$

$$E_{\text{tot}} = \frac{-\mu m}{2a} + \int \varepsilon I_{\text{avg}} dt + \int \vec{\omega}_{\text{earth}} \cdot (\vec{r} \times \vec{F}_{\text{ed}}) dt + \int \vec{F}_{\text{drag}} \cdot d\vec{s} . \quad (2.6)$$

The change in the total energy for each timestep can be given by

$$\Delta E_{\text{orb}} = \Delta E_{\text{elec}} + \Delta E_{\text{earth}} + \Delta E_{\text{drag}} . \quad (2.7)$$

This change gives the amount of orbital energy being transferred to other subsystems. If the energy transfer is maximized to the electrical subsystem while minimizing the transfer to other subsystems, then the maximum amount of energy can be stored for performing orbit maneuvers with the satellite.

Orbital debris, consisting of defunct satellites, spent rocket stages, and fragments from collisions, presents a potential energy source that can be harnessed for satellite operations. By intercepting and capturing debris, their kinetic energy can be converted into electrical energy using innovative harvesting technologies. A spacecraft equipped with an EDT can rendezvous with space debris to strategically repurpose the debris' embodied orbital energy into electrical energy while deorbiting it.

The concept of debris-based energy harvesting aligns with principles of sustainability and resource utilization in space exploration. Rather than considering debris solely as a hazard to be mitigated, this approach transforms debris into a valuable energy resource, contributing to the resilience and self-sustainability of satellite operations. Moreover, advancements in debris energy harvesting technologies could lead to innovative solutions for debris mitigation and spacecraft propulsion. Research and development efforts in this field could pave the way for more efficient and sustainable space missions, reducing reliance on traditional power sources and enhancing the resilience of satellite systems in Earth's orbit.

2.4 Energy and Power

In orbital mechanics, energy is a fundamental concept used to describe the state of a spacecraft in orbit. The energy of an orbit is determined by factors such as the mass of the spacecraft, the size of the orbit (semi-major axis), and the gravitational influence of the celestial body around which the spacecraft orbits. The formula $\frac{\mu m}{2a}$ quantifies the energy associated with the orbit, where μ represents the standard gravitational parameter (GM_{earth}), m is the mass of the spacecraft, and a is the semi-major axis of the orbit. This energy value provides insights into the stability and characteristics of the orbit.

On the other hand, in electrical systems, power plays a central role in describing the flow and conversion of energy. Power (P) is the rate at which energy is transferred or converted, and it is calculated based on variables such as current I , voltage V , and resistance R . The relationship between these variables is expressed through

$$P = IV = \frac{V^2}{R} = I^2R . \quad (2.8)$$

When comparing orbital energy to electrical power, it is important to establish a common basis for analysis. This may involve converting between energy and power units or finding analogous relationships between the variables in each system. Such comparisons can provide valuable insights into the dynamics and behaviors of both orbital and electrical systems.

TeMPEST identifies seven sources of electrical energy, namely anode, tether load, thrust, storage, cathode, and plasma [20]. To simplify the analysis, load, thrust, and storage can be neglected. It is important to note that thrust and storage will never operate simultaneously because of the opposite functionality of both the devices, i.e., storage will trap the energy, whereas the thruster uses that same energy to boost the orbit.

2.4.1 Anode

For this research, a Parker-Murphy conducting sphere (passive contactor) is considered.

The current collected can be given using a modified Parker-Murphy formula

$$i_{pm}(v) = I_0 \alpha_{pm} \left[1 + \left(\frac{V_{pm}}{\Phi_0} \right)^{\beta_{pm}} \right], \quad (2.9)$$

where

$$I_0 = \frac{\pi}{2} r_{pm}^2 q n_e \sqrt{\frac{8k_B T_e}{\pi m_e}}, \quad (2.10)$$

$$\Phi_0 = \frac{q r_{pm}^2 B^2}{8m_e}, \quad (2.11)$$

in which, r_{pm} is the radius of the sphere, B is the magnitude of ambient magnetic field, and q , n_e , k_B , T_e , and m_e are the charge, electron density, Boltzmann constant, electron temperature, and electron rest mass, respectively. The power dissipated by the anode is

$$P_{\text{anode}} = i_{pm} V_{pm}, \quad (2.12)$$

where the voltage, V_{pm} is found using an iterative method.

2.4.2 Cathode

For the simulations, a hollow cathode plasma contactor (HCPC) is considered. The power dissipated at the cathode can be given as

$$P_{\text{cathode}} = i_{\text{bare_end}} V_{\text{cathode}}, \quad (2.13)$$

where $i_{\text{bare_end}}$ is the current that flows through the plasma contactor before leaving into the surrounding plasma.

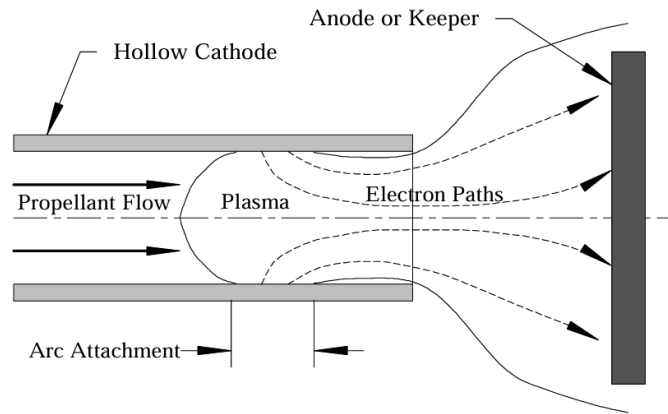


Figure 2. Schematic of an Open-Cathode Hollow Contactor [28]

2.4.3 Load

A load can be given to the tether to limit the current flow as well as to represent a generic power-consuming device like on-board scientific instruments, a transmitter, or a control device.

The load power is assumed to follow the general I^2R relation

$$P_{\text{load}} = i_{\text{end}}^2 R_L . \quad (2.14)$$

The load was set to zero for the simulations to obtain the maximum possible energy values. To simulate a real-life satellite mission with critical onboard devices, the bare load resistance was set to 120Ω .

2.4.4 Tether

The total power dissipated across the tether is given by the sum of the power dissipated in each segment given by

$$P_{\text{tether}} = \sum_n p b_n , \quad (2.15)$$

where $pb_n = (ib_n)^2 dR_t d_{len}$ in which ib_n is the current in a segment, dR_t is the resistance of the tether per length, and d_{len} is the length of the segment of the tether.

2.4.5 Thrust

The simulations run for this research are in energy harvest mode (de-boost mode). Hence, the thruster is always turned off and, therefore, does not contribute to the total electrical power and energy. If the voltage generated by the on-board power supply exceeds the voltage generated by the induced electromotive force, then the current will flow in the direction opposite to flow expected during harvest mode, which will result in the boost of the orbit.

2.4.6 Storage Device

Assuming a generic storage device with a fixed voltage regardless of current flowing through it, the power contribution from the generic energy storage device can be given as

$$P_{\text{storage}} = i_{\text{end}} V_{\text{storage}} \quad . \quad (2.16)$$

2.4.7 Total Electrical Power and Electrical Energy

The total electrical power can be written as

$$P_{\text{elec}} = P_{\text{anode}} + P_{\text{cathode}} + P_{\text{storage}} + P_{\text{load}} + P_{\text{tether}} \quad . \quad (2.17)$$

For the EDT system, it can be deduced that the voltage driving the current is the motional EMF.

Hence, the total electrical power can also be written as

$$P_{\text{elec}} = P_{\text{EMF} \times I} = \varepsilon I , \quad (2.18)$$

where ε is the EMF and I is the current.

Assuming no energy being transferred to subsystems other than the electrical subsystem in Equation 2.7, a relation between orbital and electrical energy can be derived through conservation of energy, i.e.,

$$\Delta E_{\text{orbital}} = E_{\text{electrical}} = \varepsilon I \Delta t , \quad (2.19)$$

which can be expanded into

$$\frac{\mu m}{2} \left(\frac{1}{a_2} - \frac{1}{a_1} \right) = (P_{\text{anode}} + P_{\text{cathode}} + P_{\text{storage}} + P_{\text{load}} + P_{\text{tether}}) \Delta t . \quad (2.20)$$

In conclusion, the total energy generated by the electrodynamic tether system can also be given by calculating the electrical energy by using the relationship shown in Equation 2.19 for each time step.

Chapter 3

Tether Composition and Simulation Software

3.1 Composition of Tether System

An electrodynamic tether system consists of the following:

- a conductive wire (tether) that is either bare or insulated,
- a contactor/emitter,
- an end-mass, and
- a satellite with which the tether is attached to.

The sections below go into detail about the functionality of each component along with the reasoning behind the desired configuration selected for the simulation.

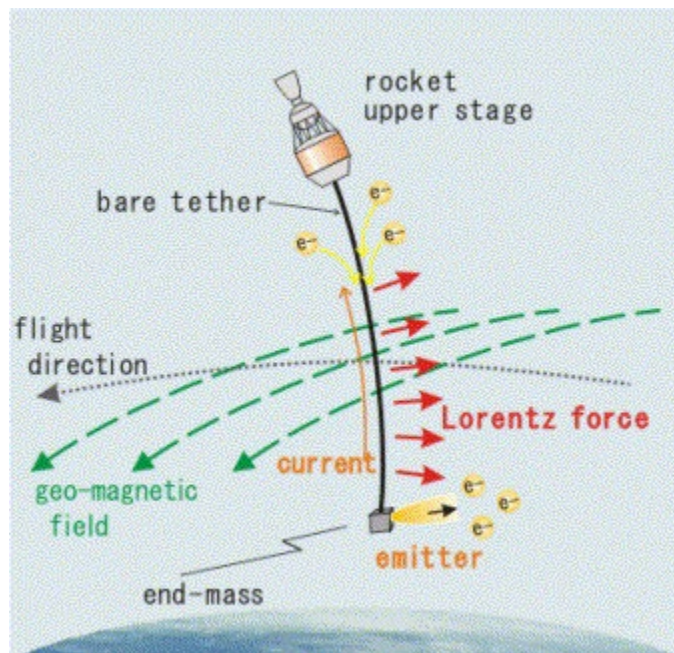


Figure 3. Schematic of an Electrodynamic Tether operating in Earth's magnetic field [29]

3.1.1 Tether Insulation

Conductive tethers can be configured in two primary ways: insulated and bare, and combinations thereof. An insulated tether has an insulation that can be made of a non-conductive material preventing direct contact between the conductive material and the surrounding ionosphere. As a result, the current along the length of the tether remains unaffected by external charges. Instead, the current flow is determined by traditional factors such as resistivity, diameter, length, and temperature. In contrast, bare tethers are exposed to the surrounding plasma environment. This exposure allows for a dynamic interaction between the tether and the ions and electrons in the plasma. If a segment of the bare tether holds a higher voltage compared to the surrounding plasma, it attracts electrons, leading to an influx of electron current into the tether. Conversely, if the segment holds a lower voltage, it attracts ions. When an ion collides

with the tether, it can draw an electron away, resulting in an electron current flowing out of the tether. This interaction between the tether and the surrounding plasma adds a dynamic component to the current. For this study, a bare tether configuration was chosen for simulations since it is known that bare tethers outperforms fully or even partially insulated tethers when operating in a high electron density plasma region [21].

3.1.2 Material Composition

The material composition of a space tether is vital for its effectiveness in diverse space missions. Traditional choices like copper and aluminum offer good strength and low electrical resistance, while tungsten provides an alternative with excellent strength and moderate conductivity, suitable for specific mission requirements. Cutting-edge materials such as carbon nanotubes (CNTs) and graphene, along with composite options like carbon fiber composite offer tailored solutions, balancing strength, weight, and electrical conductivity to meet the demands of space exploration.

This research solely focuses on utilizing aluminum for space tether simulations. Although alternative materials like carbon fiber composites and CNTs offer intriguing possibilities due to their exceptional strength-to-weight ratios and high conductivity, aluminum stands out for its reliability and balanced properties of strength and conductivity as well as being available in abundance and cheaper to mold into conductive wires. By exclusively exploring aluminum-based tether configurations in simulations, the aim is to thoroughly evaluate their performance across diverse conditions, enabling informed design decisions and maximizing the effectiveness of space tether systems.

3.1.3 Tether Geometry

Space tether designs vary widely, ranging from simple single strands to more complex braided configurations resembling electrical wiring in a house, which can be insulated or bare. In 2020, York University in Toronto launched a 100-m-long conducting bare-tape tether, another tape design to be considered for conductive tethers, on board of a payload comprising two 1U CubeSats.

Modern research into alternative designs includes the development of thin and wide tape configurations, which can be made lighter by incorporating an array of small holes to increase structural stability and maximize mass-equivalent electron current collection. Because of its remarkable characteristics, the $C_{12}A_7:e^-$ electride has previously been proposed as one of the most favorable materials for applying coatings to Low Work-function Tethers (LWTs) [22]. Additionally, there is another design called Hoytether design, which utilizes a computer-controlled weaving process to interlace copper strands into a lattice pattern, enhancing tether survivability against micrometeoroid impacts and other space debris [27]. In this design, multiple strands work in tandem to redistribute load in the event of a severed line, ensuring continued functionality and mission success.

3.1.4 Plasma Contactors

A plasma contactor is a device used in spacecraft to manage the electrical charge that builds up on its surface due to interactions with the space environment. This charge buildup can cause issues such as electrostatic discharge, which can damage sensitive spacecraft components. Plasma contactors help mitigate these issues by emitting ionized gas (plasma) to neutralize the

spacecraft's charge. The flow of current in the tether depends on the interface between the ends of the tether and the surrounding plasma and, hence, a contactor can be used to help facilitate the flow of electrons or ions between the spacecraft and the ionosphere.

A contactor can be either active or passive. Active plasma contactors utilize electrical power to ionize gas and emit ions into space. They actively generate and control plasma, providing precise charge neutralization. Passive plasma contactors, on the other hand, rely on natural processes such as photoemission or thermionic emission to produce ions. They do not require external power sources, but may have less control over the emitted ions compared to active contactors.

3.1.4.1 Thermionic Cathode Plasma Contactor

Thermionic cathode plasma contactors (TCPCs) utilize the principle of thermionic emission, where electrons are emitted from a heated cathode surface. These emitted electrons ionize the surrounding gas, creating a plasma cloud that neutralizes the spacecraft's charge.

3.1.4.2 Hollow Cathode Plasma Contactor

Hollow cathode plasma contactors (HCPCs) consist of a hollow tube containing a cathode. A current is passed through the cathode, heating it, and causing ionization of the gas inside the tube. This ionized gas forms the plasma cloud used for charge neutralization.

3.1.4.3 Parker-Murphy Sphere

The Parker-Murphy plasma contactor employs a combination of thermionic and photoemission processes. It utilizes a heated filament (thermionic cathode) in combination with ultraviolet radiation (photoemission) to produce ions for charge neutralization.

3.1.4.4 Field Emitter Cathode

Field emitter cathodes (FECs) use high electric fields to extract electrons from a cathode surface. These emitted electrons ionize the surrounding gas, generating a plasma cloud for charge neutralization.

3.1.4.5 Electron Cyclotron Resonance Plasma Contactor

An electron cyclotron resonance (ECR) plasma contactor utilizes strong magnetic fields to trap electrons and accelerate them to high energies. When these high-energy electrons collide with neutral gas atoms, they ionize them, creating a plasma cloud for charge neutralization. ECR plasma contactors offer efficient charge neutralization and can operate in low-pressure environments.

3.1.4.6 Radio Frequency Plasma Contactor

Radio frequency (RF) plasma contactors use radio frequency power to ionize gas and create plasma. By applying RF power to an antenna or electrode, the gas surrounding the

spacecraft is ionized, forming a plasma cloud. RF plasma contactors offer precise control over plasma density and can be adjusted to accommodate different mission requirements.

Each type of plasma contactor has its advantages and disadvantages in terms of efficiency, control, and power consumption, making them suitable for different spacecraft applications and mission requirements. For the simulations in this research, TeMPEST uses HCPC model and Parker-Murphy for calculating the cathode and anode voltage respectively in energy harvest mode.

3.1.5 End-mass

An end-mass is a component of an EDT system attached to one end of the tether. Passive end-masses stabilize the system with their mass alone, relying on gravitational and inertial forces. They are simple and lack propulsion or control mechanisms. Active end-masses, on the other hand, are more complex by incorporating propulsion and control systems to actively maneuver and control the tether dynamics. They can adjust their position and velocity relative to the tether, providing more precise control and allowing for tasks like tension adjustment, attitude control, or orbital maneuvers.

3.1.6 Energy Storage Devices

Energy storage devices are vital components of satellites, ensuring continuous power availability during periods of eclipse or when the solar panels are not receiving sunlight. Various

types of energy storage devices are utilized in satellites, each with its unique characteristics and applications.

3.1.6.1 Batteries

Batteries are the most common energy storage devices on satellites. They store electrical energy chemically and release it as needed. Rechargeable batteries, such as nickel–cadmium (NiCd), nickel–hydrogen (NiH₂), and lithium–ion (Li–ion) batteries, are favored due to their ability to be charged and discharged multiple times. NiCd batteries are robust and have been extensively used in space missions, although their energy density is relatively low compared to newer technologies like Li–ion batteries, which offer higher energy density and longer lifespan.

3.1.6.2 Supercapacitors

Supercapacitors, also known as ultracapacitors or electric double-layer capacitors (EDLCs), store energy electrostatically rather than chemically. They can charge and discharge rapidly, making them suitable for applications requiring high-power bursts. While supercapacitors have lower energy density compared to batteries, they excel in delivering quick energy surges, such as during satellite maneuvers or payload operations.

3.1.6.3 Flywheels

Flywheel energy storage systems store energy in the rotational motion of a spinning mass. They offer high power density and fast response times, making them suitable for

applications requiring rapid energy storage and retrieval. Flywheels are particularly advantageous for satellites requiring frequent attitude control adjustments. However, they typically have lower energy density compared to batteries and supercapacitors.

3.1.6.4 Thermal Energy Storage

Thermal energy storage (TES) systems utilize phase change materials (PCMs) to store and release energy through changes in their physical state, such as melting and solidification. TES devices are primarily used for thermal management purposes on satellites, storing excess heat generated by onboard electronics during periods of sunlight and releasing it when needed to maintain optimal operating temperatures.

Each type of energy storage device has its advantages and limitations, and the choice depends on factors such as mission requirements, power demands, weight constraints, and reliability considerations. Typically, satellites employ a combination of these devices to ensure redundancy and optimize power management throughout their operational lifespan.

3.2 TeMPEST

TeMPEST, the TEthered Mission Planning and Evaluation Software Tool, was first developed at the University of Michigan's Space Physics Research Laboratory (UM/SPRL) in 1994 to support the Tethered Satellite System (TSS-1R) mission. Initially designed to simulate tether behavior in space, it predicted induced voltages and collected currents based on system

configuration, orbital parameters, magnetic fields, and plasma conditions. Since then, it has evolved and expanded its capabilities, with ongoing development and utilization at various institutions including UM/SPRL, Tethers Unlimited, Inc. (TUI), ElectroDynamic Applications, Inc. (EDA), and The Pennsylvania State University.

3.2.1 History of TeMPEST

In 1994, the development of TeMPEST was initiated at UM/SPRL in support of the reflight of the Tethered Satellite System (TSS-1R) to be able to simulate the behavior of a tether system in space [20]. The initial purpose of the TeMPEST tool was to realistically predict the induced tether voltages and collected tether currents of the TSS-1R mission based on the tether system configuration, spacecraft orbital parameters, local magnetic field, and ambient plasma to aid in the planning of the mission and training of instrument operators. Subsequently, TeMPEST was found to be useful for other EDT concepts, and its feature set and capabilities have been continually improved and expanded. TSS-1 and TSS-1R flight data were used to validate TeMPEST simulation results. Over the years, TeMPEST has been used to study various tethered systems and support tethered satellite system development and has evolved to include various features to help in generating more accurate results [23].

3.2.2 General Architecture

TeMPEST initializes the simulation by reading in command line arguments and a separate parameter file. This file contains all the user inputs that are unique to the simulation

including, but not limited to, initial time, initial orbital characteristics, tether properties, contactors, energy storage parameters, and system properties. The command line arguments generally deal with file outputs and debug flags. After reading the command line and the parameters file, a check for “bad input” is performed and initial variables (such as the initial orbital energy) are set. Next, the module dependencies are adjusted to ensure that only the relevant modules will be activated for the simulation parameters chosen. If, for example, one wishes to calculate energy storage, then environmental modules such as ionospheric plasma, EMF, and magnetic field modules must be activated as well as general orbit, tether, and atmospheric neutral density modules.

Chapter 4

Results and Analysis

4.1 System Concept

The purpose of this simulation is to show that EDT systems can be used as secondary or even as a primary source of energy for small-size satellites or a smallsat at higher inclination. According to NASA, “smallsats typically weigh under 180 kg and are the size of a large kitchen fridge.” Hence, for simulation purposes, the total mass of the satellite system (including tether mass) is assumed to be 200 kg. Discussed below are the details about tether components allocated towards the design of the energy harvesting system.

4.1.1 Tether

Building upon the insights from Section 3.1.1, this research adopts a bare tether configuration. Specifically, an aluminum tether is selected, as detailed in Section 3.1.2, for its suitability in the intended application. The tether simulation is conducted across varying lengths, spanning from 1 to 4 km. Notably, the study examines three primary wire gauges: 15 AWG, 25

AWG, and 30 AWG. It is important to determine if a tether can fit inside the satellite. Let's consider that we have a compartment size of 25 cm × 25 cm × 25 cm available for storing the tether coil inside the smallsat. Using a simple mathematical formula, one can determine if a 4-km, 15-AWG bare tether can fit inside of the given space.

$$L_w = \frac{\pi (OD^2 - ID^2)}{4 \frac{T}{1000}}, \quad (4.1)$$

where OD, ID, and T are the outer and inner diameter of the coil (in meters) and the thickness of the wire (in mm), respectively. For maximum capacity, considering an inner diameter of 5 mm, a total length of 33.84 m is obtained. Stacking 172 of these coils gives us a total length of 5820.5 m. Hence, a 4-km, 15-AWG bare tether can fit inside the given space.

4.1.2 Orbital Parameters

For simplicity purposes, 39 out of the 50 SMC objects discussed in Section 2.1 were grouped into four groups of objects with similar orbital parameters (like apogee, perigee, and inclination) and mass as detailed in Table 2. The averaged orbital parameters of these groups were then used to set orbital parameters into four different parameter files to run simulations.

Table 2. SMC objects distributed into four main groups

GROUP 1							
SATNO	SATNAME	Apogee, km	Perigee, km	Incl, deg	Mass, kg	Country	Launch Date
22566	SL-16 R/B	848	837	71	9000	CIS	3/26/1993
22220	SL-16 R/B	848	827	71	9000	CIS	11/17/1992
31793	SL-16 R/B	846	843	71	9000	CIS	6/29/2007
26070	SL-16 R/B	854	827	71	9000	CIS	3/2/2000
16182	SL-16 R/B	844	833	71	9000	CIS	10/22/1985
20625	SL-16 R/B	853	834	71	9000	CIS	3/22/1990
23705	SL-16 R/B	852	831	71	9000	CIS	10/31/1995
25407	SL-16 R/B	844	835	71	9000	CIS	7/28/1998
23405	SL-16 R/B	845	838	71	9000	CIS	11/24/1994
17974	SL-16 R/B	846	823	71	9000	CIS	5/13/1987
23088	SL-16 R/B	845	841	71	9000	CIS	4/23/1994
22285	SL-16 R/B	844	840	71	9000	CIS	12/25/1992
22803	SL-16 R/B	850	823	71	9000	CIS	9/16/1993
19650	SL-16 R/B	848	831	71	9000	CIS	11/23/1988
24298	SL-16 R/B	863	839	70.8	9000	CIS	4/9/1996
28353	SL-16 R/B	848	842	71	9000	CIS	10/6/2004
17590	SL-16 R/B	841	831	71	9000	CIS	3/18/1987
19120	SL-16 R/B	842	814	71	9000	CIS	5/15/1988
AVG.		847.83	832.72	70.99	9000		

GROUP 2							
SATNO	SATNAME	Apogee, km	Perigee, km	Incl, deg	Mass, kg	Country	Launch Date
23704	COSMOS 2322	854	842	71	3250	CIS	10/31/1995
28352	COSMOS 2406	863	844	71	3250	CIS	10/6/2004
23087	COSMOS 2278	852	841	71	3250	CIS	4/23/1994
19119	COSMOS 1943	851	833	71	3250	CIS	5/15/1988
17973	COSMOS 1844	866	824	71	3250	CIS	5/13/1987
20624	COSMOS 2082	856	833	71	3250	CIS	5/22/1990
AVG.		857.00	836.17	71.00	3250		

GROUP 3							
SATNO	SATNAME	Apogee, km	Perigee, km	Incl, deg	Mass, kg	Country	Launch Date
10732	SL-8 R/B	995	966	82.9	1435	CIS	3/15/1978
21090	SL-8 R/B	992	961	82.9	1435	CIS	5/2/1991
10693	SL-8 R/B	989	957	83	1435	CIS	2/28/1978
7594	SL-8 R/B	981	955	82.9	1435	CIS	12/26/1974
23180	SL-8 R/B	992	950	82.9	1435	CIS	7/14/1994
10138	SL-8 R/B	1001	970	82.9	1435	CIS	8/7/1977

13917	SL-8 R/B	996	954	82.9	1435	CIS	3/24/1983
14625	SL-8 R/B	999	969	82.9	1435	CIS	11/1/1984
12092	SL-8 R/B	996	953	82.9	1435	CIS	10/12/1980
9044	SL-8 R/B	988	966	83	1435	CIS	7/21/1976
16292	SL-8 R/B	996	953	82.9	1435	CIS	11/28/1985
AVG.		993.18	959.45	82.92	1435		

GROUP 4							
SATNO	SATNAME	Apogee, km	Perigee, km	Incl, deg	Mass, kg	Country	Launch Date
24277	ADEOS	794	793	98.9	3560	JPN	8/17/1996
27601	H-2A R/B	836	734	98.2	3000	JPN	12/14/2002
24279	H-2 R/B	1306	860	98.7	2700	JPN	8/17/1996
27597	ADEOS 2	801	800	98.5	3680	JPN	12/14/2002
AVG.		934.25	796.75	98.58	3235.00		

4.1.3 Assumptions

For the electrodynamic system, it is assumed that the tether is rigid and it is aligned with the local gravity gradient. It is also assumed that there are no tether librations. Another assumption being made in the simulation is regarding the energy. As mentioned in Section 2.3, to maximize the orbital energy being converted into electrical energy, it is important to minimize the energy being transferred to other subsystems. Hence, one can assume the total change in the orbital energy gives the electrical energy that can be used by the satellite to boost the orbit or can be stored in an energy storage device.

4.2 Results

4.2.1 Mission Elapsed Time (Lifetime)

When operating in harvesting mode, an electrodynamic tether system experiences a gradual loss of altitude. This phenomenon stems from the interaction between the current flowing through the tether and the Earth's geomagnetic field as discussed in Section 2.2. Figure 4 shows the decrease in altitude (in ECI-frame) measured from the center of the Earth over the entire mission time. The rate of altitude loss correlates directly with the magnitude of the current; hence, a larger current leads to a swifter de-orbiting of the satellite system. As the satellite descends closer to Earth's surface, it encounters heightened electron density, resulting in increased power generation, as illustrated in Section 4.3.3. Notably, electron density diminishes below 300 km altitude, which leads to a steeper decrease in the altitude as can be seen in Figure 4.

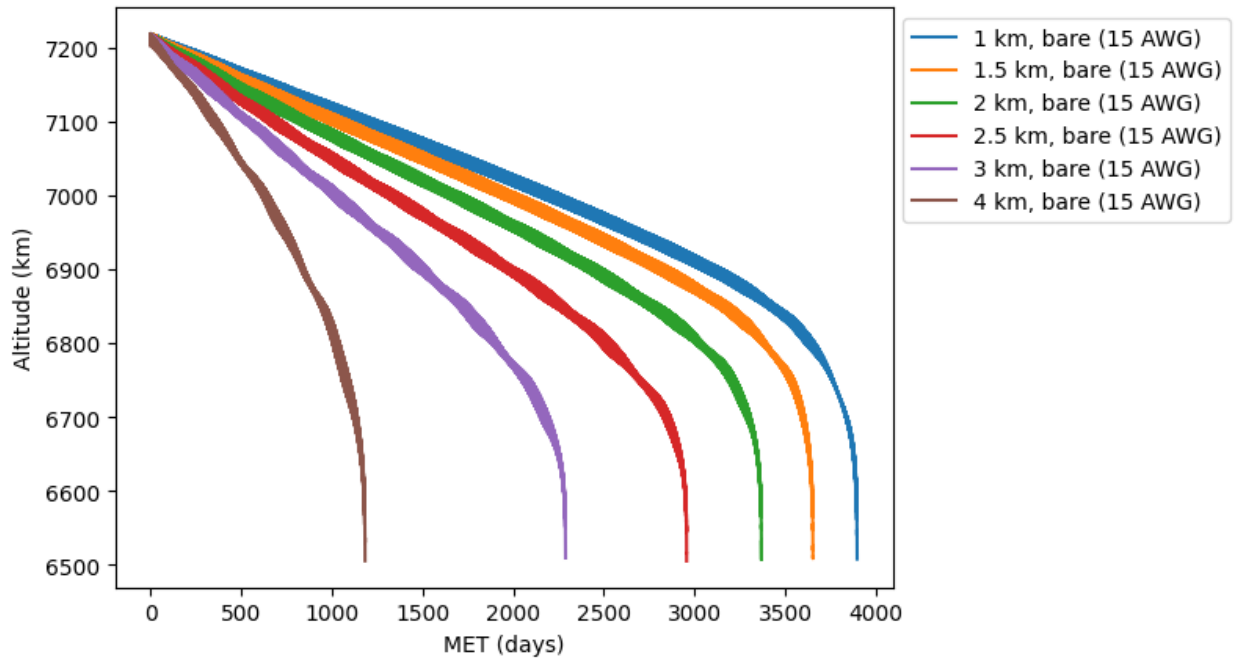


Figure 4. Altitude versus mission elapsed time for Group1 orbit

4.2.2 Total Energy

As shown in Figure 5, the 15-AWG bare tether has the potential of generating more energy than the other two gauge configurations being considered due to less resistance, which leads to higher current flow. Note that, to obtain maximum energy, load resistance was assumed to be 0Ω . In Figure 6, the total energy generated throughout the mission lifetime for a 3-km-long bare tether is almost double that generated by a 1-km-long bare tether. There is not much difference in the total energy generated by a 3-km and a 2.5-km tether during its mission lifetime. It is important to note that, as the length of the tether increases, the rate of generation of energy (electrical power) increases rapidly. Hence, for a mission that requires high energy output such as missions that require rapid orbital adjustments, a 4-km-long tether can be an optimum choice. Whereas missions with sustained, low-thrust applications, can use a 1-km-long tether.

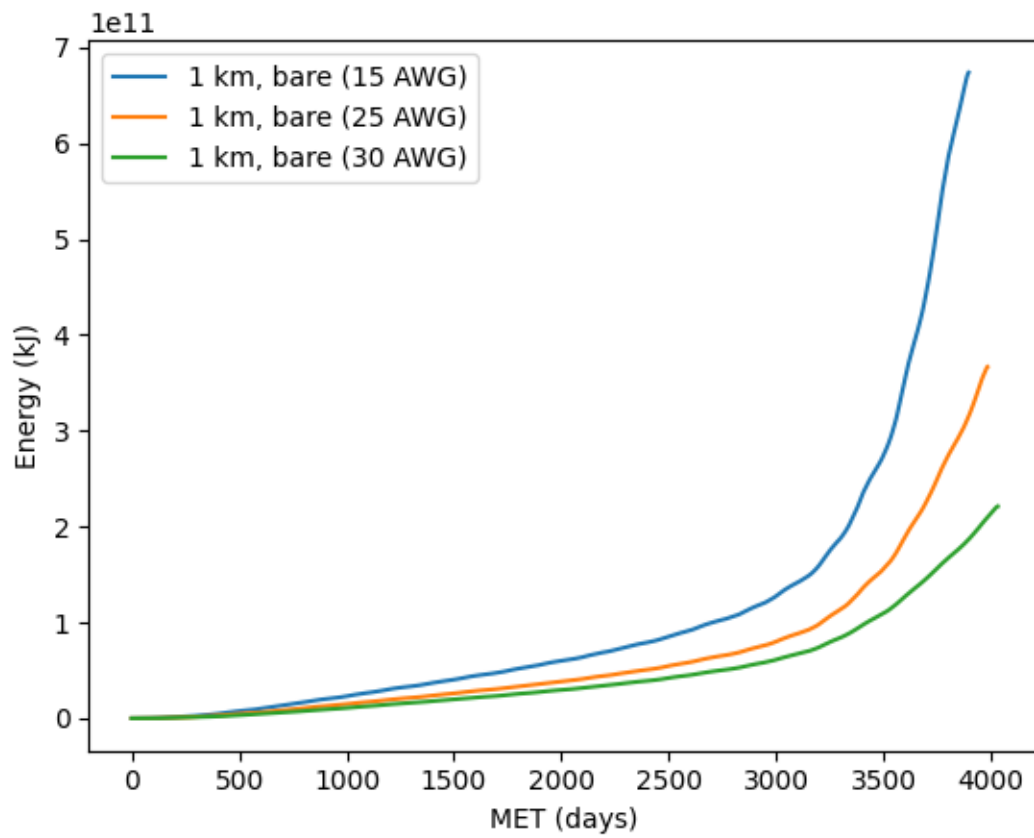


Figure 5. Total energy versus mission elapsed time for various tether diameters for Group1 orbit

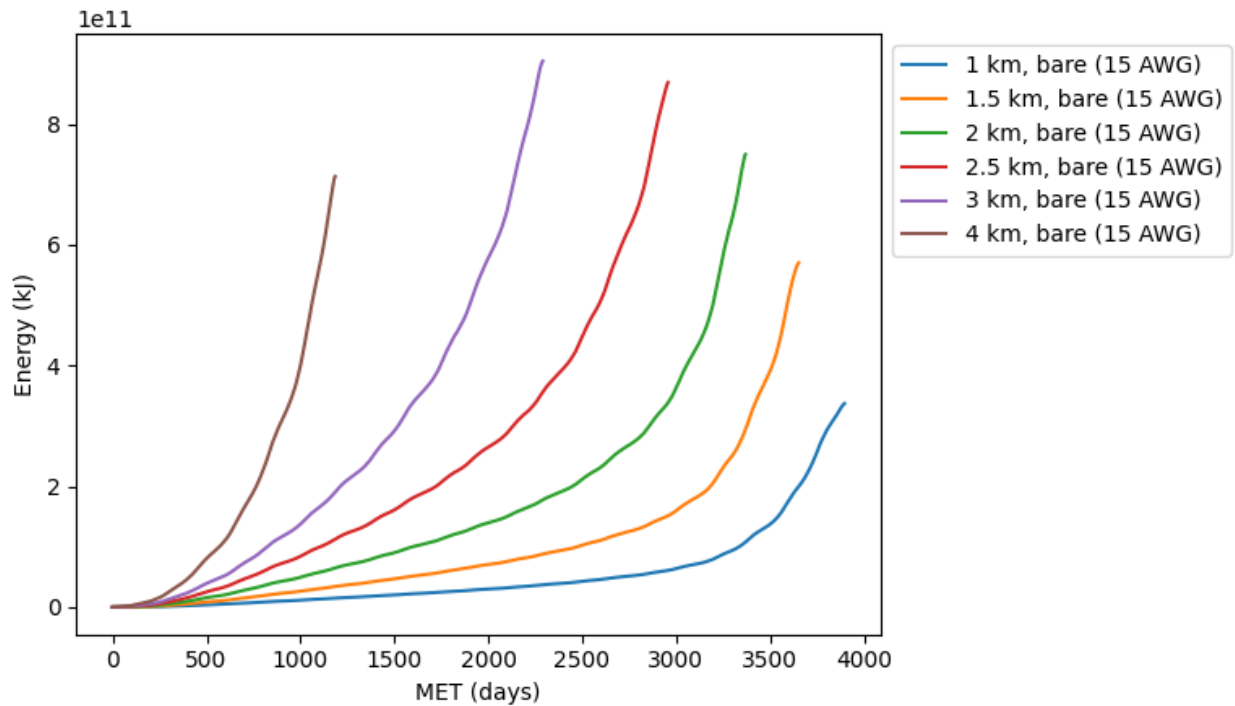


Figure 6. Total energy versus mission elapsed for various tether lengths for Group1 orbit

4.2.3 Power

When the inclination exceeds 60 degrees, the strength of the magnetic field decreases rapidly, resulting in lower power generation compared to lower inclinations. As shown in Figure 7, power generation remains below 10 W for most of the mission's duration. Small satellites are commonly used for purposes like communication, Earth observation, and surveillance, typically needing 50–100 W of power for critical onboard functions. Initially, an additional power source will be necessary to supply energy to onboard devices. However, once enough energy is stored, it can be used to power other devices onboard.

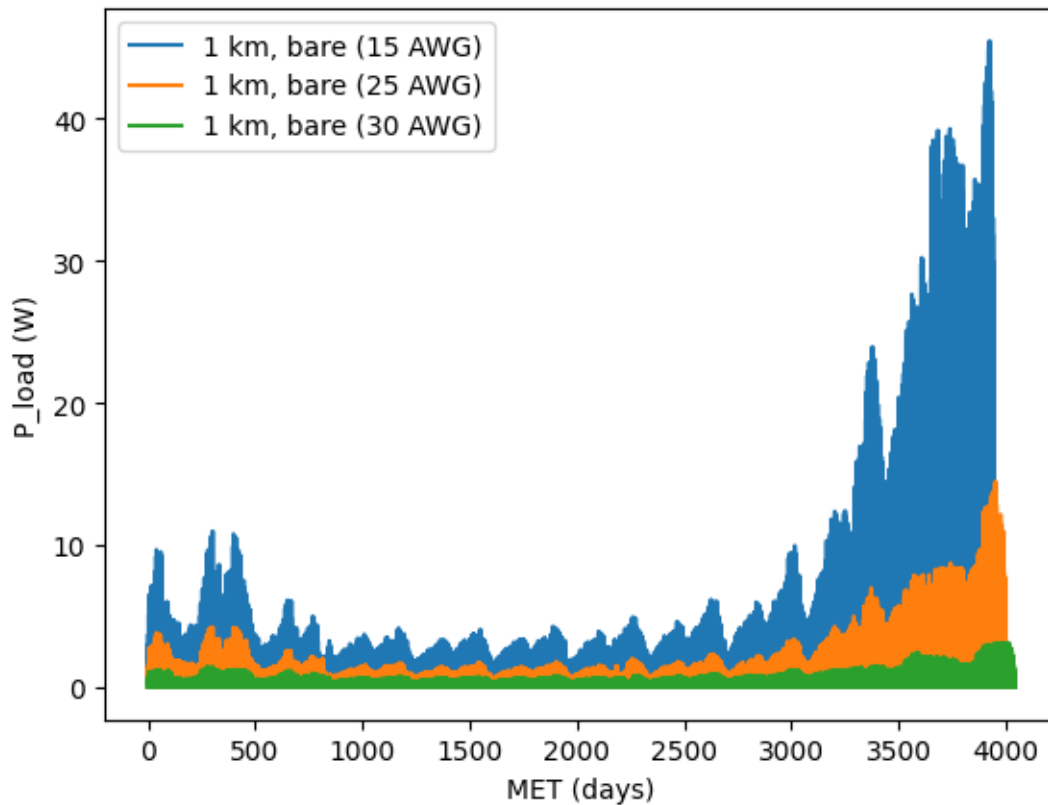


Figure 7. Power as a function of mission elapsed time for Group1 orbit

4.3 Summary

In conclusion, the results demonstrate the viability of EDT systems for small satellite missions, offering potential benefits such as altitude control and enhanced power generation. Moreover, these systems could expand satellite capabilities by incorporating functions like debris mitigation. These findings suggest promising avenues for future research and development in the field of space technology, paving the way for more efficient and versatile small satellite missions.

Chapter 5

Conclusion and Future Work

In the pursuit of enhancing the capabilities of small satellite missions, this study has delved into the feasibility and potential benefits of employing EDT systems as primary or secondary energy sources. Through simulation and analysis, a comprehensive understanding of the system's functionality, performance characteristics, and operational implications has been attained.

The investigation began with a conceptual overview of EDT systems, highlighting their role in energy harvesting and altitude control for small satellites. By exploring various tether configurations, including different lengths and wire gauges, the study provided valuable insights into design considerations and compatibility within the constraints of small satellite platforms.

Moreover, by grouping SMC objects based on similar orbital parameters, the study facilitated a realistic assessment of system performance under diverse operational conditions. This approach enabled a nuanced understanding of the interplay between tether dynamics and orbital mechanics, essential for optimizing system efficiency.

While acknowledging the assumptions and limitations inherent in simulation, the study underscored the importance of optimizing energy transfer and minimizing interference with other

subsystems to maximize operational efficiency. Through detailed analysis of mission elapsed time, total energy generation, and power output across different scenarios, the study elucidated the performance characteristics and operational implications of EDT systems.

The implications of this research extend beyond theoretical exploration, offering practical insights and avenues for future investigation. The findings affirm the viability of EDT systems for small satellite missions, demonstrating their potential to address critical needs such as altitude control and power generation. Moreover, EDT systems hold promise for augmenting satellite capabilities, enabling functions such as debris mitigation and extended mission lifetimes through efficient energy management.

Future research endeavors could focus on refining simulation software to incorporate the missing energy storage module in TeMPEST, and also to enhance the overall performance of TeMPEST to simulate various configurations of tether systems like adding plasma contactors models to simulate modern plasma contactors, add the framework for energy storage devices to automate the de-boost and re-boost process to simulate a real-life tether system with energy storage device, and exploring novel applications to further enhance the performance and versatility of EDT systems. Integrating these systems into small satellite missions will require collaboration between researchers, engineers, and space agencies to address technical challenges, regulatory considerations, and operational requirements.

In conclusion, the analysis presented in this study underscores the potential of EDT systems as transformative elements in small-satellite missions. By harnessing the principles of electromagnetic induction and orbital dynamics, these systems offer a compelling solution for enhancing energy efficiency, maneuverability, and operational longevity in space. As the space industry continues to evolve, leveraging EDT technology presents exciting opportunities for

advancing space exploration, satellite deployment, and scientific research. Through continued innovation, collaboration, and exploration, the possibilities for unlocking the full potential of electrodynamic tether systems in space missions are boundless.

Bibliography

[1] Angelo, J. A., *Space Technology*. Greenwood Publishing, Westport, Conn, USA, 2003.

[2] Pelt, M. V., *Space Tethers and Space Elevators*, Springer, Berlin, Germany, 2009.

[3] Beletsky, V. V., and Levin, E. M., *Dynamics of Space Tether Systems*, Advances in the Astronautical Sciences, American Astronautical Society, Washington, DC, USA, 1993.

[4] Isaacs, J. D., Vine, A. C., Bradner, H., and Bachus, G. E., "Satellite Elongation into a True 'Sky-hook'," *Science*, Vol. 151, No. 3711, 1966, pp. 682–683.

[5] Colombo, G., Gaposchkin, E. M., Grossi, M. D., and Weiffenbach, G. C., "The Sky-hook: A Shuttle-borne Tool for Low-orbital-Altitude Research," *Meccanica*, Vol. 10, No. 1, 1975, pp. 3–20.

[6] Pearson, J., "The Orbital Tower: A Spacecraft Launcher using the Earth's Rotational Energy," *Acta Astronautica*, Vol. 2, No. 9-10, 1975, pp. 785–799.

- [7] Moravec, H., “A Non-synchronous Orbital Skyhook,” *Journal of the Astronautical Sciences*, Vol. 25, No. 4, 1977, pp. 307–322.
- [8] Pearson, J., “Anchored Lunar Satellites for Cislunar Transportation and Communication,” *Journal of the Astronautical Sciences*, Vol. 27, No. 1, 1979, pp. 39–62.
- [9] Bergamaschi, S., Bonon, F., Merlina, P., and Morana, M., “Theoretical and Experimental Investigation of TSS-1 Dynamics,” *Acta Astronautica*, Vol. 34, No. C, 1994, pp. 69–82.
- [10] Li, G., Spence, L., Miller, M., Pandya, M., Stankey, N., Hancock, A., Lu, R., Park, C., Rajesh, A., Beloiu, A., and Gilchrist, B., “Lessons Learned from the Development and Flight of the First Miniature Tethered Electrodynamic Experiment (MiTEE-1),” *35th Annual Small Satellite Conference*, 2021.
- [11] Bilén, S. G., Stone, N., Scadera, M., Fuhrhop, K. P., Elder, C. H., Hoyt, R. P., Gilchrist, B. E., Alexander, L., Wiegmann, B. M., and Johnson, C. L., “The Propel Electrodynamic Tether Mission and Connecting to the Ionosphere,” *12th Spacecraft Charging and Technology Conference*, 2012. <https://ntrs.nasa.gov/citations/20120015031>.
- [12] Estes, R. D., Lorenzini, E. C., Sanmartin, J. R., Pelaez, J., Martinez-Sanchez, M., and Johnson L., “Bare Tethers for Electrodynamic Spacecraft Propulsion,” *Journal of Spacecraft and Rockets*, Vol. 37, No. 2, 2000, pp. 205–211.

[13] Weis, L., and Peck, M., “Attitude Control for Chip Satellites using Multiple Electrodynamic Tethers”, *AIAA/AAS Astrodynamics Specialist Conference*, AIAA 2012-4871, 2012.

doi:10.2514/6.2012- 4871

[14] Hudoba de Badyn, M., Marchand, R., and Sydora, R. D., “Using Orbital Tethers to Remediate Geomagnetic Radiation Belts”, *JGR Space Physics*, Vol. 121, No. 2, Jan. 2016, pp. 1114-1123. doi:10.1002/2015JA021715

[15] Janhunen, P., “Electric Sail for Spacecraft Propulsion,” *Journal of Propulsion and Power*, Vol. 20, No. 4, 2004, pp. 763–764. doi: 10.2514/1.8580

[16] Huang, P., Zhang, F., Cai, J., Wang, D., Meng, Z., and Guo, J., “Dexterous Tethered Space Robot: Design, Measurement, Control, and Experiment,” *IEEE Transactions on Aerospace and Electronic Systems*, Vol. 53, No. 3, 2017, pp. 1452–1468.

[17] Bischof, B., Kerstein, L., Starke, J., Guenther, H., and Foth, W.P., “ROGER-robotic Geostationary Orbit Restorer,” *Science and Technology Series*, Vol. 109, 2004, pp. 183–193.

[18] Liu, Y., Liu, X., Cai, G., Xu, F., and Tang, S., “Detumbling a Non-Cooperative Tumbling Target Using a Low-Thrust Device,” *AIAA Journal*, Vol. 60, No. 5, 2022, pp. 2718–2729.

[19] McKnight, D., et al., “Identifying the 50 Statistically-most-concerning Derelict Objects in LEO,” *Acta Astronautica*, Vol. 181, 2021, pp. 282–291. doi:10.1016/j.actaastro.2021.01.021.

- [20] McTernan, J. K., “Development of a Modeling Capability for Energy Harvesting Modules in Electrodynamic Tether Systems,” M.S. Thesis, Aerospace Engineering, The Pennsylvania State University, 2011.
- [21] Fuhrhop, K. R., and Gilchrist B. E., “Electrodynamic Tether System Analysis Comparing Various Mission Scenarios,” 41st AIAA/ASME/SAE/ASEE Joint Propulsion Conference and Exhibit, AIAA-2005-4435, 2005.
- [22] Fabian-Plaza, J., Meiro, G., Post, A., Pérez-Casero, R., Palomares, F. J., Tejedor, P., Naghdi, S., Várez, A., and Sánchez-Arriaga, G., “Trade-off Analysis of C12A7:e- Deposition Techniques Applied to Low Work Function Tethers,” *Acta Astronautica*, Vol. 177, Dec. 2020, pp. 806–812.
- [23] Sanmartin, J.R., Lorenzini, E.C. and Martinez-Sanchez, M., “Electrodynamic Tether Applications and Constraints”, *Journal of Spacecraft and Rockets*, Vol. 47, No.3, 2010, pp. 442–456. doi:10.2514/1.45352
- [24] NASA - NSSDCA - *Spacecraft - Details*. Available at:
<https://nssdc.gsfc.nasa.gov/nmc/spacecraft/display.action?id=TSS-1> (Accessed: 23 April 2024).
- [25] Carroll, J. A., “Guidebook for Analysis of Tether Applications,” *NASA Contractor Report*, NASA CR-178904, 1985.

[26] *Orbital Debris Quarterly News*, Vol. 26, No.4, NASA, Nov. 2022, pp. 14.

[27] Hoyt, R. P., Slostad J., and Twiggs R., “The Multi-Application Survivable Tether (MAST) Experiment,” 39th AIAA/ASME/SAE/ASEE Joint Propulsion Conference and Exhibit, AIAA-2003-5219, 2003.

[28] Domonkos, M.T., “Evaluation of Low-Current Orificed Hollow Cathodes,” PhD Dissertation University of Michigan, 1999.

[29] Kawamoto, S., Makida, T., Sasaki, F., Okawa, Y., and Nishida, S., “Precise Numerical Simulations of Electrodynamic Tethers for an Active Debris Removal System,” *Acta Astronautica*, vol. 59, Apr. 2006, pp. 139–148.

Appendix A

Simulation Graphs

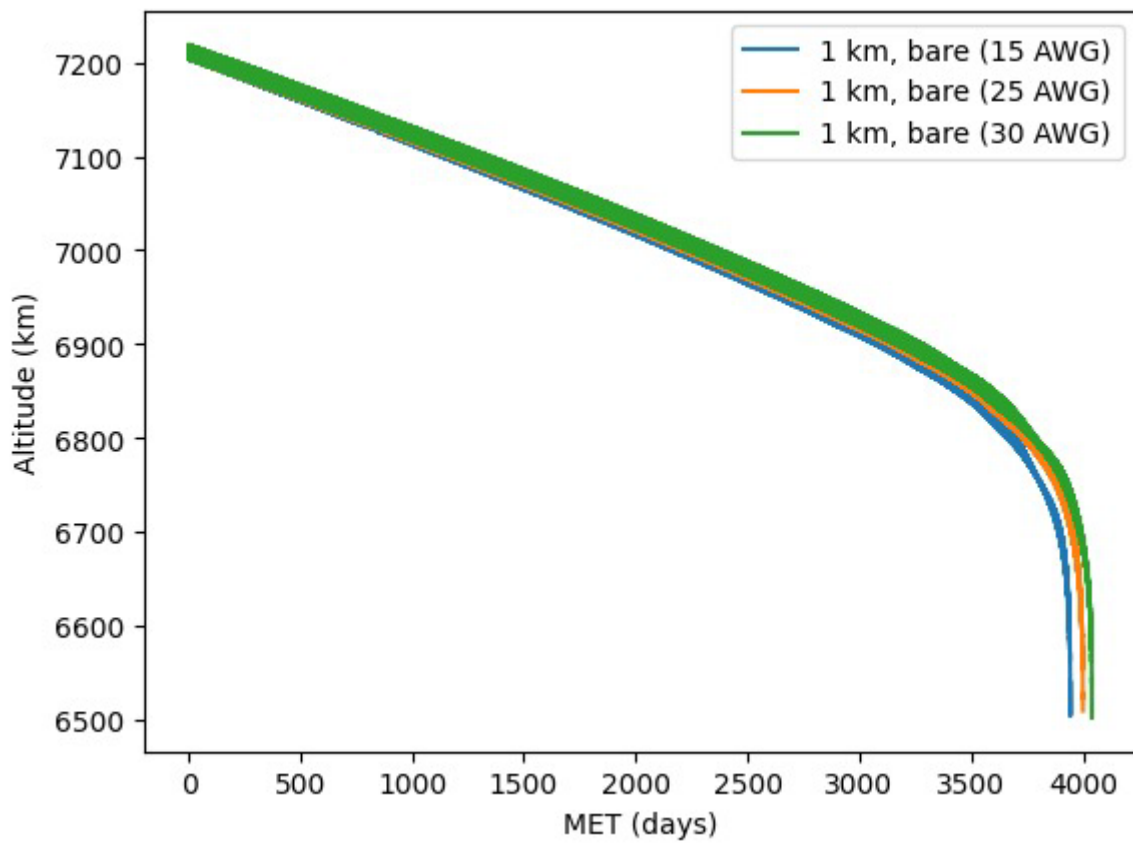


Figure 8. Altitude versus mission elapsed time for Group1 orbit (Load resistance = 100 Ω)

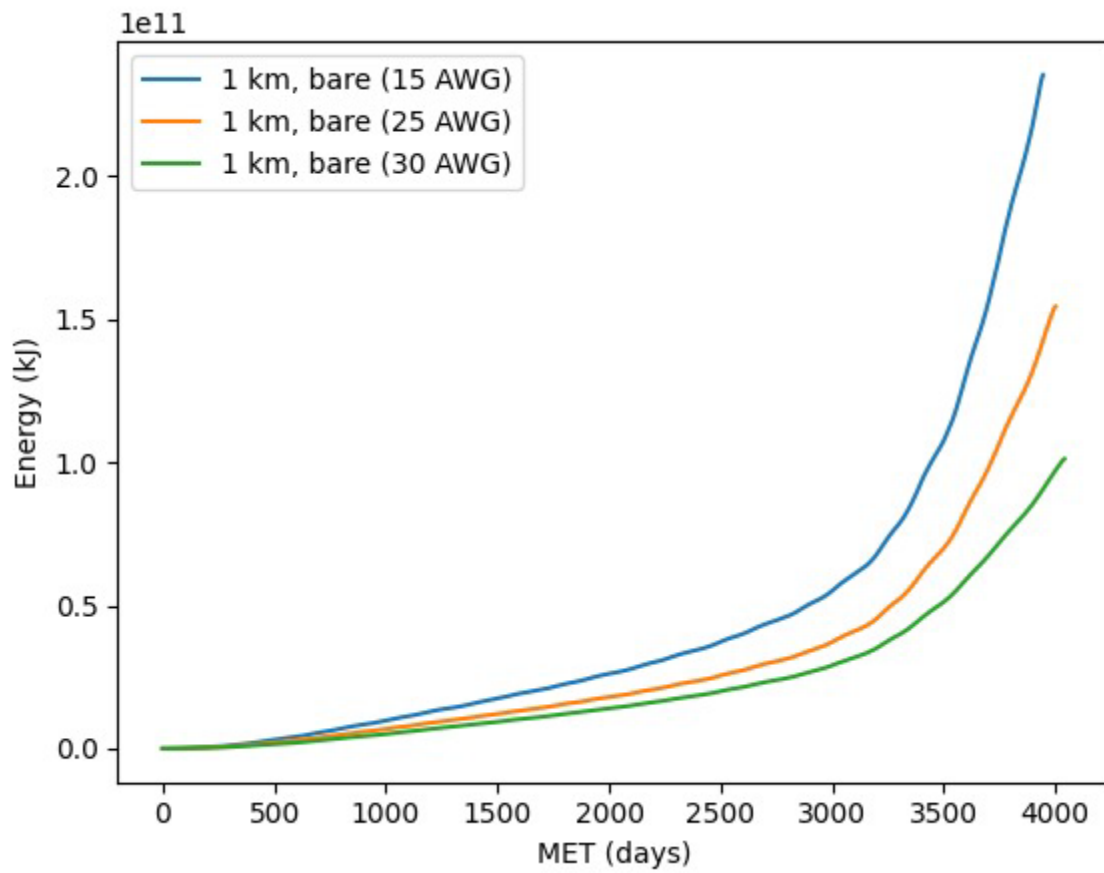


Figure 9. Energy versus mission elapsed time for Group1 orbit (Load resistance = 100Ω)

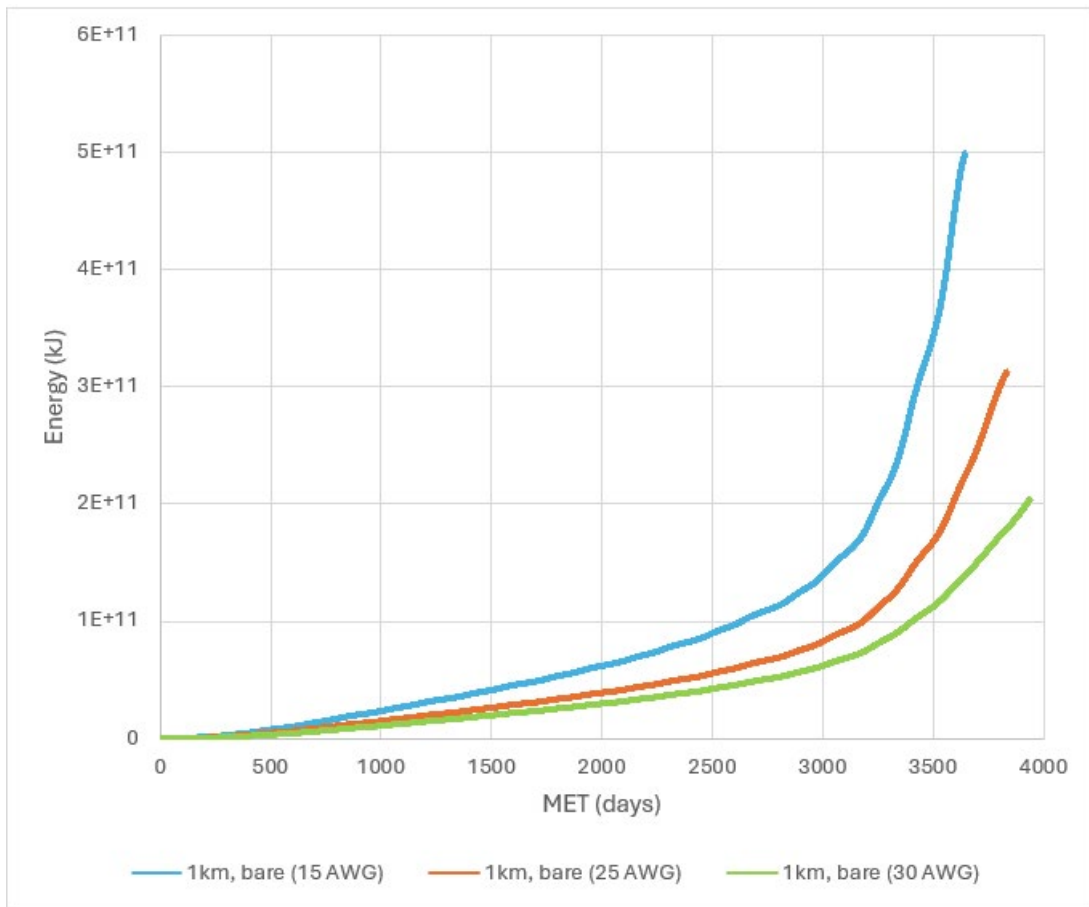


Figure 10. Energy versus mission elapsed time for Group2

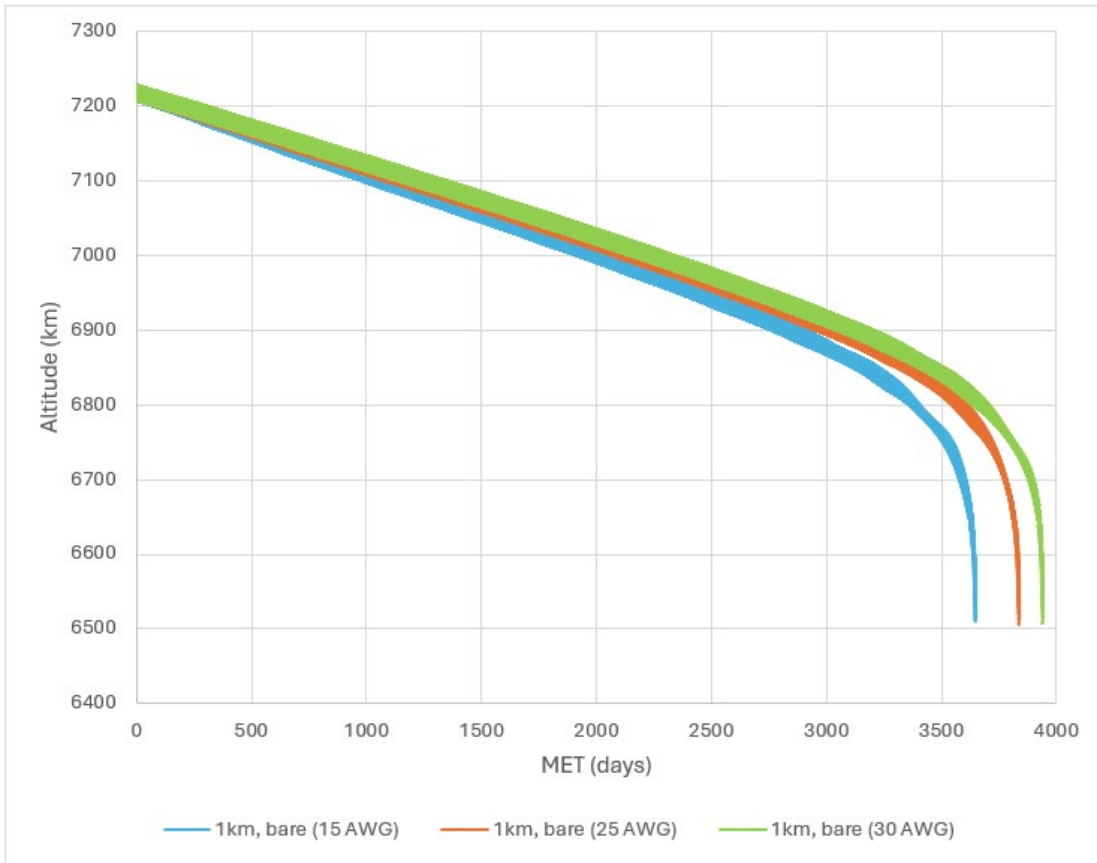


Figure 11. Altitude versus mission elapsed time for Group2

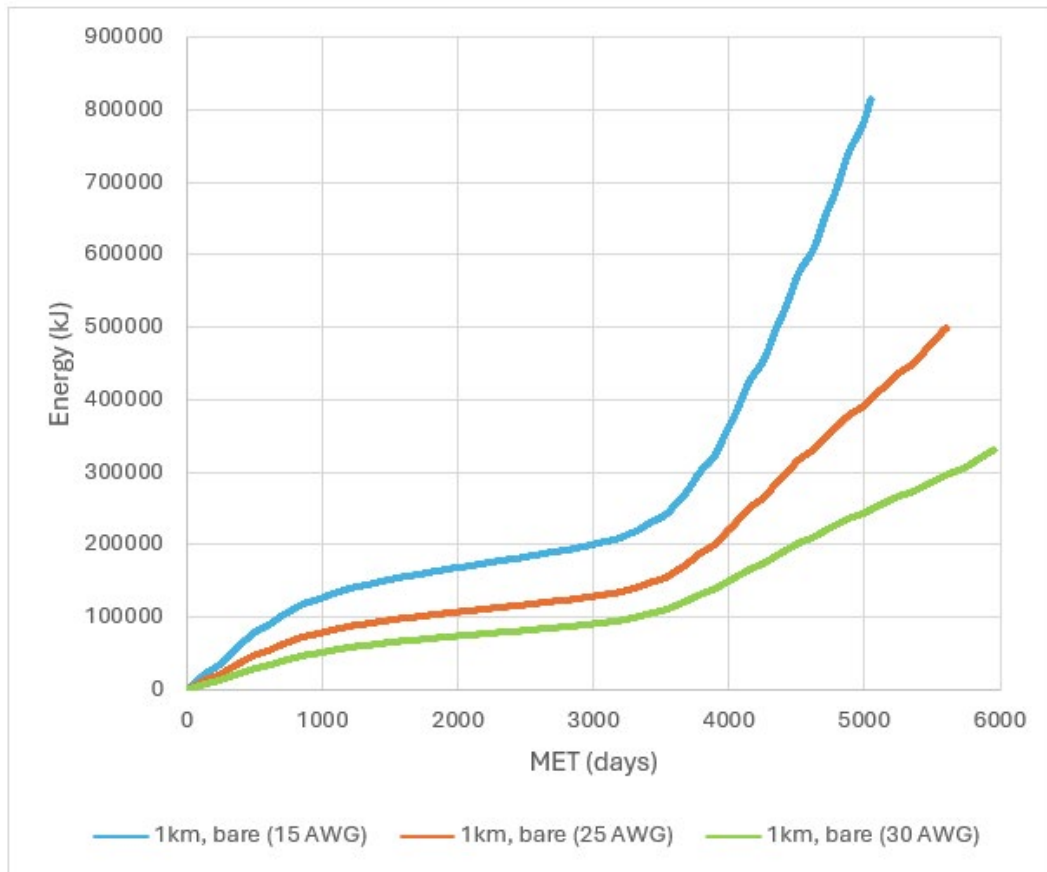


Figure 12. Energy versus mission elapsed time for Group3

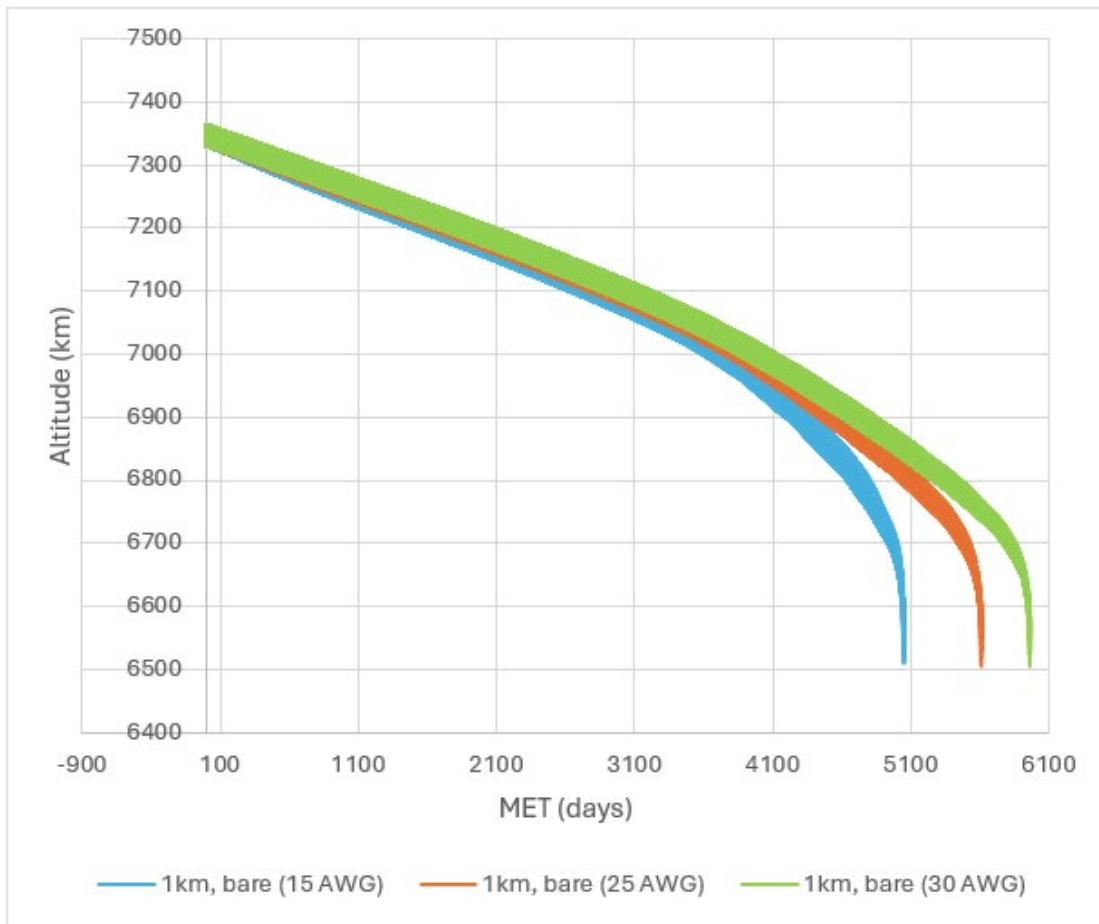


Figure 13. Altitude versus mission elapsed time for Group3

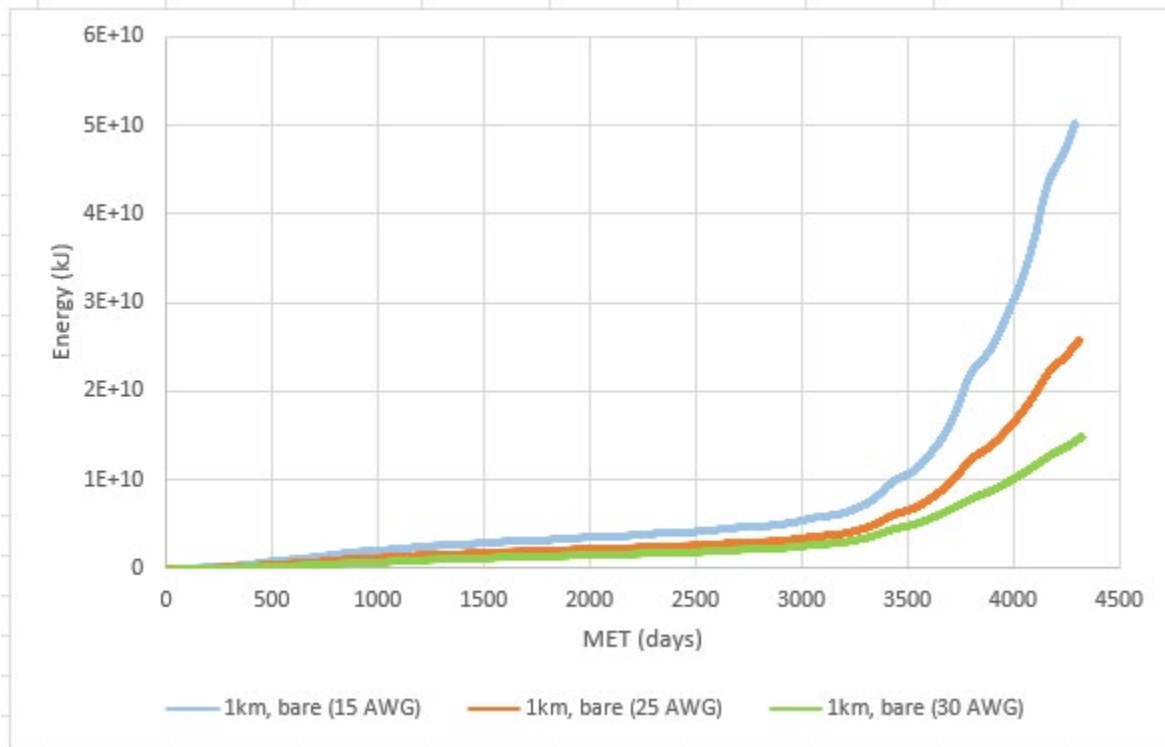


Figure 14. Energy versus mission elapsed time for Group4

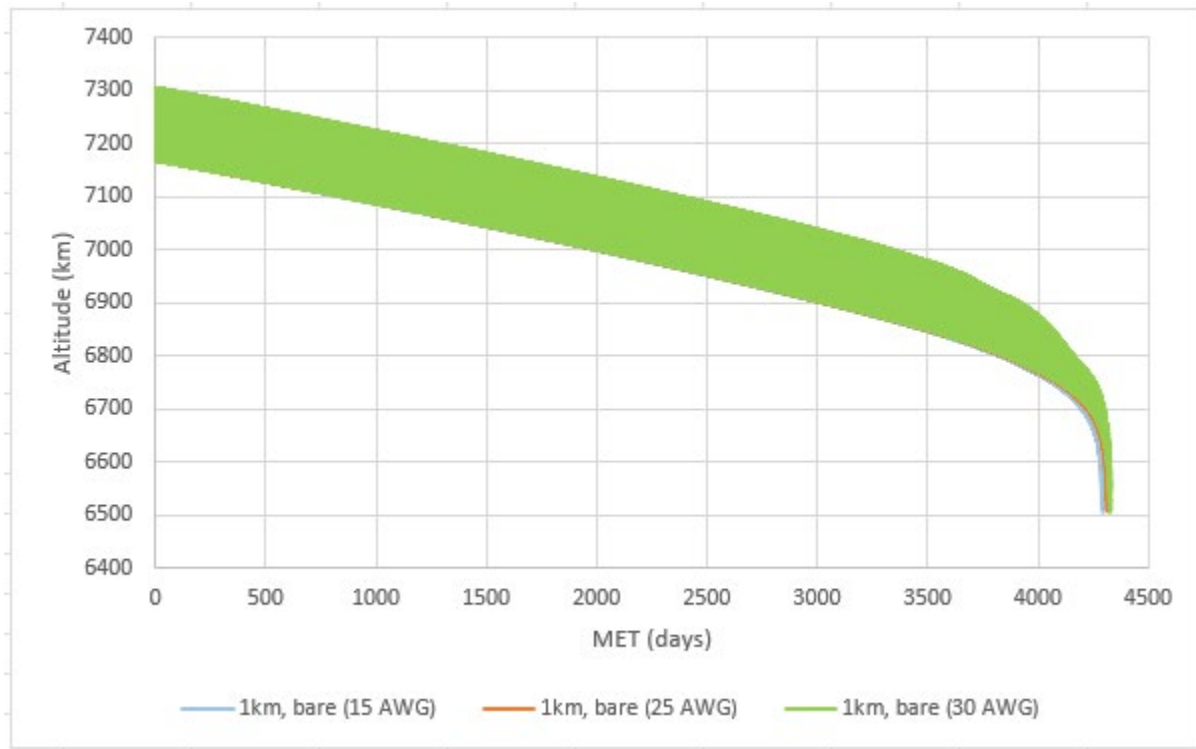


Figure 15. Altitude versus mission elapsed time for Group4

Appendix B

Sample Parameters File

```

# Aluminum, 1km bare (15 AWG)
#### EPOCH PARAMETERS ####
Ephemeris_Year = 2000
Ephemeris_Time = 001/00:00:00

APOGEE_ALT      = 847830 # height above earth radius (in m)
PERIGEE_ALT     = 832720 # height above earth radius (in m)
Inclination     = 70.99
RAAN            = 0.0
Arg_Perigee    = 0.0
Anomaly_Type    = True
True_Anomaly    = 0.0
System_mass     = 9500 # mass of entire tether system (in kg) (do
                      not forget to add s/c +tether mass)

##### Simulation Parameters #####
Orbit_Perturb   = Yes
Orbit_Decay     = Yes
Orbit_Precise   = Yes
Ephem_From_RV  = Yes

##### NO libration (EMFgg = EMFlib) #####
InPlane_Lib    = 0.00
OutofPlane_Lib = 0.00
Radial_Lib     = 0.00
IP_Phase       = 0.00
OP_Phase       = 0.00
Rad_Phase      = 0.00

##### Simulation Start & Stop Time #####
Start_Year     = 2000
Start_Time     = 001/00:00:00.000
Stop_Year      = 2020
Stop_Time      = 001/00:00:00.000
##### METO Time = Launch time #####
METO_Year      = 2000
METO_Time      = 001/00:00:00.00

```

```

#####
###
# Increment by 30 seconds
Time_Incr = 000/00:02:00.000
SS_Output = 10

#####
###
# Set tether length to 'upward deployed' (HARVEST MODE)
# 1 km, bare
Tether_End      = 1000.0
Bare_Start      = 000.0
Bare_End        = 1000.0
T_Resistivity   = 0.00000282 # ohms * cm (Aluminum)
T_Cond_Radius   = 0.000725   # meters (15 AWG)

Bare_Segments   = 1000
Bare_Load       = 0.0        # Ohms

##### Upper Contactor
#####
# anode (collects electrons)
# PM sphere (2)
# Ohms Law (4) --> V=P1*I^P2+P3
#   P1 =R, P2 =power of 1, P3 =0 (constant)
#   Use P1 =small number for ideal anode (e.g, 0.000001)

Contactor_UP    = 2
pm_r_sat        = 1.0        # sat radius in m
pm_alpha        = 2.5
pm_beta         = 0.52

# Initial guess for Anode Bias
Anode_Bias      = 400.0

#####
###
# HCPC for lower body contactor
# P1=Molecular weight of expellant (Xenon = 131.29)
# P2=Gas flow rate in SCCM
# P3=Double Layer Voltage Drop (e.g. 4.0V)
# P4=Source Te (e.g 3.889)

Contactor_Down  = 7
Contactor_P1_Dn = 131.29
Contactor_P2_Dn = 0.5

```

```
Contactor_P3_Dn = 4.0
Contactor_P4_Dn = 3.889

# Initial Guess for Cathode Bias
Cathode_Bias    = -400.0

#####
###
# List out outputs

Show_Vars = MET_DAYS
Show_Vars = P_LOAD
Show_Vars      = R_ECI
Show_Vars      = V_ANODE
Show_Vars      = V_CATHODE
Show_Vars = I_BARE_AVE
Show_Vars = EMF_INDUCED
```

Ritu Bhalodia

717-6082011 | bhritu34@gmail.com | <https://www.linkedin.com/in/ritu-bhalodia-aviation-enthusiast>

EDUCATION

Bachelor of Science: Aerospace Engineering

The Pennsylvania State University

Dec 2019- May 2024

Schreyer Honors College - University Park, PA

SKILLS

- Proficient in, CATIA V5, SolidWORKS, Siemens NX, ANSYS-FEA/CFD, C++, MATLAB/Simulink
Linux/C language, Arduino, Python, PCB Design and Circuit Prototyping
- Participated in sports like Taekwondo, Judo, Bojutsu and Volleyball

WORK EXPERIENCE

Research/Internship

Structural and Mechanical Engineering Intern

May 2023- Present

Boeing

- Designed and performed stress analysis on 777-8F Intercostal
- Reviewed Finite Element Modeling of floor beams for 777-8F program
- Working on Stanchion stress analysis for 77-8F program

Undergraduate Research

Feb 2022- Present

Space Propulsion Laboratory, University Park, PA

- Conducted research on the effects of micro-meteorite strikes into Earth's ionosphere using a Low Earth Orbit (LEO) vacuum chamber
- Modified various aspects of the vacuum system, including the cold-head, compressor, electronics system, gas flow, and plasma source to define boundary conditions for the experiment
- Working on Electrodynamic Tether (EDT) Systems simulation using Linux-based software Program to gain a better understanding of how Tethers work in space.

Systems Engineering Intern

Sept 2022- Dec 2022

GE Aerospace

- Collaborated with the Advance Technologies Operation (ATO) Team to work on the CFM Open-fan Engine Demonstrator
- Designed and built an instrumentation package for the Ground Test Demo (GTD)
- Served as the systems lead for test enabling hardware for the GTD, effectively contributing to the successful completion of the project.

NASA L'SPACE

Jan 2022- Aug 2022

NASA Proposal Writing and Evaluation Experience

- Developed outlines, strategies, and persuasive content for proposals while overseeing the proposal development process from kickoff to submission
- Acquired hands-on experience working with industry professionals to collaborate on NASA-related team projects while learning about NASA mission procedures and protocols
- Established successful partnerships with NASA, Arizona State University, and NASA Goddard Space Flight Center, effectively contributing to the success of team projects and initiatives.

Research Assistant

Jan 2022- May 2022

Collins Aerospace Project, VLRCOE, University Park, PA

- Collaborated on Durable Deicing Coating System Hybrid with Heat Protection System
- Worked on redesigning the Deicing Testing Chamber at VLRCOE lab

- Designing and building airfoil-shaped testing coupons for durable deicing coating test

Multi-campus Research Experience for Undergraduates

Summer 2021-22

University Park, PA

- Conducted research on Fabrication and Characterization of CNT-Reinforced Second-Generation Al-Matrix Composites
- Evaluated the graphs generated by Spectrophotometer used for testing the absorption of CNTs-surfactant solutions
- Generated aluminum flaky powders using CNC mill

Leadership

Peer Tutor Coordinator

Jan 2022- Present

Penn State Learning, University Park, PA

- Interviewing math tutor candidates for Penn State Learning
- Preparing scheduled shifts for all the Math Tutors
- Monitoring peer tutors' performances from time-to-time

Corporate Liaison

Jan 2022- May 2023

Penn State SASE

- Collaborated with companies to host events for our General Body Members
- Raised \$ 10k for sponsorship for the club